Folia Hort. 36(1) (2024): 35–66

DOI: 10.2478/fhort-2024-0003

FOLIA HORTICULTURAE

Published by the Polish Society for Horticultural Science since 1989

ORIGINAL ARTICLE | Open access | https://sciendo.com/journal/FHORT

Zinc oxide and silver effects on the growth, pigment content and genetic stability of chrysanthemums propagated by the node culture method

Alicja Tymoszuk[1,*], *Urszula Szałaj*[2], *Jacek Wojnarowicz*[2], *Jolanta Kowalska*[3], *Małgorzata Antkowiak*[3], *Dariusz Kulus*[1]

[1] Laboratory of Horticulture, Department of Biotechnology, Faculty of Agriculture and Biotechnology, Bydgoszcz University of Science and Technology, Bernardyńska 6, 85-029 Bydgoszcz, Poland
[2] Laboratory of Nanostructures, Institute of High Pressure Physics, Polish Academy of Science, Sokołowska 29/37, 01-142 Warsaw, Poland
[3] Department of Organic Agriculture and Environmental Protection, Institute of Plant Protection–National Research Institute, Władysława Węgorka 20, 60-318 Poznań, Poland

ABSTRACT

This article describes benefits of the application of zinc oxide submicron particles (ZnO SMPs), zinc oxide nanoparticles (ZnO NPs) and ZnO NPs combined with silver NPs (ZnO + Ag NPs) in chrysanthemum micropropagation. Single node explants of *Chrysanthemum* × *morifolium* (Ramat.) Hemsl. 'UTP Burgundy Gold (UBG)' and 'UTP Pinky Gold (UPG)' were inoculated on the Murashige and Skoog (MS) medium and treated with 100 mg · L^{-1}, 200 mg · L^{-1}, or 400 mg · L^{-1} ZnO SMPs, ZnO NPs (1.5% H_2O), ZnO NPs (6% H_2O), ZnO + 0.1% Ag NPs (1.5% H_2O), ZnO + 0.1% Ag NPs (6% H_2O), ZnO + 1% Ag NPs (1.5% H_2O) and ZnO + 1% Ag NPs (6% H_2O). Generally, the tested materials stimulated the growth and development of plantlets. In 'UBG', the most prominent treatments affecting increases in the number of leaves, micropropagation coefficient, shoot length and shoot FW/DW weight included 400 mg · L^{-1} ZnO SMPs and 100 mg · L^{-1} ZnO NPs (6% H_2O). In 'UPG', the treatments with 200 mg · L^{-1} ZnO + 0.1% Ag NPs (6% H_2O) and 200 mg · L^{-1} ZnO + 1% Ag NPs (6% H_2O) were the most successful. The latter treatment stimulated an intensive development of root systems in the two studied cultivars. High values of leaf area, perimeter and width were reported in both cultivars for 400 mg · L^{-1} ZnO + 1% Ag NPs (6% H_2O). As compared to the control, the treated plants were characterised by a similar or, most often, lower content of chlorophylls and carotenoids. The randomly amplified polymorphic DNA (RAPD) and start codon targeted polymorphism (SCoT) marker system analyses of the 400 mg · L^{-1} ZnO SMPs/ZnO NPs/ZnO + Ag NPs-treated chrysanthemums confirmed their genetic fidelity with the control plants. The obtained results can be implemented in the commercial large-scale production of chrysanthemums.

Keywords: *Chrysanthemum* × *morifolium*, metabolites, micropropagation, nanomaterials, RAPD, SCoT

Abbreviations: DW, dry weight; FW, fresh weight; mono, monomorphic *loci*; MS, Murashige and Skoog; NPs, nanoparticles; PCR, polymerase chain reaction; poly, polymorphic *loci*; RAPD, randomly amplified polymorphic DNA; SCoT, start codon targeted polymorphism; SD, standard deviation; SMPs, submicron particles; spec, specific *loci*; ZnO NPs, zinc oxide nanoparticles; ZnO SMPs, zinc oxide submicron particles; ZnO + Ag NPs, zinc oxide nanoparticles combined with silver nanoparticles.

*Corresponding author.
e-mail: alicja.tymoszuk@pbs.edu.pl (Alicja Tymoszuk).

Open Access. © 2024 Tymoszuk et al., published by Sciendo. BY-NC-ND This work is licensed under the Creative Commons Attribution alone 3.0 License.

INTRODUCTION

Chrysanthemum × *morifolium* (Ramat.) Hemsl. is a subtropical ornamental and medicinal perennial herbaceous species belonging to the family *Asteraceae*. It has been cultivated for more than 3000 years. Chrysanthemums are among the most popular and economically important ornamental plants worldwide. They are grown undercover for cut flowers, as pot plants or in the ground – in gardening and ornamental landscaping. The popularity of this species is due to its high ornamental value, including various colours and shapes of inflorescences, and exceptionally long and uniform flowering period (Park et al., 2015; Su et al., 2019). Chrysanthemum inflorescences are also used as herbal medicines included in some pharmacopoeias and food (tea, beverages, vegetables) due to their bioactive constituents and pharmacological activities (Gu et al., 2022; Hao et al., 2022).

Plant tissue culture provides a rapid and reliable system for the production of a large number of genetically uniform and disease-free plantlets in controlled laboratory conditions, in a small space, in a short time and regardless of seasonality (Regni et al., 2022). Due to the high popularity and demand for chrysanthemum, it has become one of the first commercial targets for micropropagation. Chrysanthemum is propagated *in vivo* vegetatively through either root suckers or terminal cuttings. This conventional process of shoot cutting is very slow and time-consuming. Since cuttings are obtained repeatedly from mother plants, they can be subjected to virus infection and degeneration, thereby increasing production costs. Clonal propagation through *in vitro* culture can enhance the multiplication coefficient many fold and is utilised for large-scale propagation of healthy chrysanthemum plants (Kereša et al., 2012; Nalini, 2012). The micropropagation method with the use of single node explants (node culture method) involves a transverse division of microcuttings into fragments containing the single node and is applicable in the propagation of plants characterised by strong apical dominance, i.e. chrysanthemum. The micropropagation coefficient is, on average, four to five microcuttings per shoot (axillary shoots develop from the existing meristems on nodal explants). The node culture method is the most true-to-type method of clonal propagation applied in gene banks and large-scale plant production (Zalewska et al., 2012).

Nanotechnology is concerned with the design, synthesis, manipulation and application of atomic or molecular aggregates with a dimension between 1 nm and 100 nm. The engineering methodology and processing that produce nanoparticles (NPs) alter their physicochemical properties, as well as biological reactivity, due to nanometric size and high surface-to-volume ratio. Nanotechnology has been applied to modern agriculture and horticulture practices as innovative pesticides, fertilisers or growth stimulators (García-López et al., 2018). In recent years, the use of NPs has successfully led to the reduction of microbial contaminations in plant tissue cultures and demonstrated the positive role of NPs in callus formation, organogenesis, somatic embryogenesis, secondary metabolite production (Kim et al., 2017) and variability induction in plant breeding (Tymoszuk and Kulus, 2022).

Zinc is an indispensable plant micronutrient that controls the activity of numerous enzymes and hormones; regulates the metabolism of macromolecules, stabilising proteins, DNA and RNA structures; and controls antioxidant metabolism and gene expression. It contributes to cell proliferation and differentiation, and chloroplast development and functioning and participates in plant growth regulation affecting root and shoot development. Zinc deficiency in plants causes abnormal growth, reduced enzymatic activity and, finally, a disturbed metabolism. To fulfil the Zn requirements of plants, the smartest delivery tool for Zn may be NPs (Awan et al., 2021). Zinc in the form of zinc oxide NPs (ZnO NPs) may be more effectively absorbed by plants and increase nutrient uptake, pigment content, photosynthesis efficiency and biomass accumulation (da Cruz et al., 2019; Salachna et al., 2021; Regni et al., 2022). ZnO NPs belong to the most produced NPs worldwide and are commonly used in several industrial products such as components of solar cells, sunscreens, wall paints, ceramics, catalysis and biomedicine. ZnO NPs are also the most used NPs in agricultural applications due to easy availability, low chemical price, stability at high temperature and neutral pH (Elshoky et al., 2021; Rani et al., 2022).

ZnO NPs had a greater and more responsive impact on tobacco (*Nicotiana tabacum* L.) callus growth and physiological indices than ZnO microparticles and zinc sulphate (Mazaheri-Tirani and Dayani, 2020). Likewise, the application of ZnO NPs increased the shoot multiplication rate in the *in vitro* culture of date palm (*Phoenix dactylifera* L.) (Award et al., 2020). Media supplemented with ZnO NPs enhanced callus induction and regeneration rate in switchgrass (*Panicum virgatum* L.) (Shafique et al., 2020).

Due to unique physicochemical properties, i.e. great chemical stability, conductivity, catalytic activity and antimicrobial potential, silver NPs are the most commonly used NPs in numerous applications (Tariq et al., 2022). In plant production, they are used as plant growth stimulators, components of fertilisers and plant protection products. Ag NPs have also been used in plant tissue culture to improve seed germination and plant growth, stimulate the biosynthesis of bioactive compounds and enable genetic transformation (Mahendran et al., 2019). However, silver NPs may also show phytotoxicity, manifested by limited germination and seedling growth, decreased biomass of leaves and shoots and inhibition of photosynthesis.

Therefore, further studies are needed to clarify these contradictory observations (Salachna et al., 2019; Parzymies, 2021).

Micropropagation protocols aiming to produce efficiently true-to-type plants should guarantee the genetic fidelity of propagated plants. Since the application of NPs may result in the induction of variability, the genetic analysis of *in vitro*-propagated and NPs-treated plants is recommended (Tymoszuk and Kulus, 2022). Due to their simplicity, rapidity and versatility, genotyping methods based on polymerase chain reaction (PCR) are commonly utilised to assess the genetic variation in horticultural plants. Methods such as randomly amplified polymorphic DNA (RAPD) and start codon targeted polymorphism (SCoT) are considered powerful tools for studying the genetic diversity in chrysanthemum (Miler et al., 2023).

This study aimed to test, for the first time, the effects of ZnO NPs alone or combined with silver NPs (ZnO + Ag NPs), applied at the concentration of 100 mg · L^{-1}, 200 mg · L^{-1} or 400 mg · L^{-1}, on the growth and chlorophyll and carotenoid content, as well as genetic stability of chrysanthemums 'UTP Burgundy Gold (UBG)' and 'UTP Pinky Gold (UPG)' plantlets developed *in vitro* from single node explants. Zinc oxide submicron particles (ZnO SMPs) were also included in the study to test the effect of particle size. Since we tested a wide range of material samples with different characteristics and particle sizes, the results provide a deeper understanding of the multifaceted effects of SMPs and NPs on chrysanthemum *in vitro* at the biochemical, genetic and biometric levels and are of importance for the development of modern horticulture, both scientifically and practically. This is an innovative approach in terms of the improvement of chrysanthemum micropropagation via the node culture method, combining the achievements of nanotechnology and biotechnology.

MATERIALS AND METHODS

Materials, synthesis and characteristics of NPs

The synthesis of nanostructured ZnO NPs and ZnO + x% Ag NPs included the use of several materials such as zinc acetate dihydrate ($Zn(CH_3COO)_2 \cdot 2H_2O$, Avantor Performance Materials Poland S.A., Gliwice, Poland), silver acetate anhydrous ($Ag(CH_3COO)$, Chempur, Piekary Śląskie, Poland), ethylene glycol ($C_2H_4(OH)_2$, Chempur, Piekary Śląskie, Poland) and deionised water (H_2O) (specific conductance below 0.1 μS · cm^{-1}). All the chemical substances were analytically pure and used without further purification. SMPs of pharmaceutically pure zinc oxide (ZnO SMPs) were purchased from ZM SILESIA SA, Huta Oława, Oława, Poland.

ZnO NPs and ZnO + x% Ag NPs samples were obtained by microwave solvothermal synthesis (Wojnarowicz et al., 2020) using the authors' own procedure described in previous papers (Pokrowiecki et al., 2019; Tymoszuk et al., 2022). Briefly, to approximate the synthesis, zinc acetate dihydrate was dissolved in ethylene glycol at 70°C using a magnetic stirrer. The obtained solution was tightly sealed in a bottle. When the solution reached room temperature, the water content was analysed, and a calculated amount of water was added to reach a final water concentration of 1.5% or 6% by weight in the precursor solution. The MSS2 (Microwave Solvothermal Synthesis model 2) microwave reactor was used to synthesise the nanopowders (270 mL, 12 min, 4 bar, 3 kW, 2.45 GHz, IHPP PAN (Warsaw, Poland), ITeE-PIB (Radom, Poland) and ERTEC (Wrocław, Poland) (Majcher et al., 2013). After the synthesis, the obtained suspension was centrifuged, then the liquid from above the precipitate was decanted. The sediment was washed with distilled water and centrifuged (washing and centrifugation processes were repeated four times). The resulting paste was frozen using liquid nitrogen and dried by freeze-drying. The synthesis procedure was repeated five times, and a total of six powder samples were obtained, which were ZnO NPs (1.5% H_2O), ZnO NPs (6% H_2O), ZnO + 0.1% Ag NPs (1.5% H_2O), ZnO + 0.1% Ag NPs (6% H_2O), ZnO + 1% Ag NPs (1.5% H_2O) and ZnO + 1% Ag NPs (6% H_2O). The compositions of the precursor solutions can be found in Supplementary Table S1. Commercial submicron zinc oxide (ZnO SMPs) was used as a reference material.

The testing of the samples was carried out at the Laboratory of Nanostructures (IHPP PAN, Warsaw, Poland), which is accredited with accreditation no. AB 1503. A description of the research procedures used can be found in Wojnarowicz et al. (2018). X-ray powder diffraction (XRD) patterns were tested with an X'Pert PRO X-ray diffractometer (CuKα, Panalytical, Almelo, The Netherlands). Morphology was tested using a scanning electron microscope (ULTRA PLUS, ZEISS, Oberkochen, Germany). Skeletal density was examined using a helium pycnometer (AccuPyc II 1340, FoamPyc V1.06, Micromeritics®, Norcross, GA, USA). The specific surface area (SSA) was measured by using the Brunauer–Emmett–Teller (BET) method (Gemini 2360, V 2.01, Micromerit-ics®, Norcross, GA, USA). The zinc and the silver content were determined by energy dispersive spectrometry (Quantax 400, Bruker, Billerica, MA, USA). The water content (wt%) of the glycol solution samples was measured using the Karl Fischer method (Cou-Lo AquaMAX KF, GR Scientific, Bedford, UK).

The average crystallite size (diameter) was obtained using the Scherrer equation. The average particle size (diameter) was calculated from the skeleton density results and SSA results. The results of sample characterisation can be found in the supplementary materials (Supplementary Table S2, Supplementary Table S3 and Supplementary Figure S1). The nanopowder

samples obtained by using the microwave method were characterised by a uniform size with a homogeneous spherical shape, which was confirmed by Scanning Electron Microscopy (SEM) results (Supplementary Figure S2). For samples ZnO SMPs, ZnO NPs (1.5% H_2O), ZnO NPs (6% H_2O), ZnO + 0.1% Ag NPs (1.5% H_2O), ZnO + 0.1% Ag NPs (6% H_2O), ZnO + 1% Ag NPs (1.5% H_2O) and ZnO + 1% Ag NPs (6% H_2O), particle size was 240 nm, 25 nm, 65 nm, 29 nm, 79 nm, 27 nm and 53 nm, respectively.

Micropropagation – medium, plant material, treatments and culture conditions

For micropropagation, the modified Murashige and Skoog (MS) medium (Murashige and Skoog, 1962) was used, with the content of calcium and iron increased by half. The medium was supplemented with 30 g · L^{-1} sucrose and contained 8 g · L^{-1} Plant Propagation LAB-AGAR™ (BIOCORP, Warsaw, Poland). No plant growth regulators were used. After adding all of the nutrients, the medium pH was adjusted to 5.8. Afterwards, 40 mL of the medium was poured into 350-mL glass jars sealed with plastic caps and autoclaved (105 kPa, 121˚C, 20 min).

Two *Chrysanthemum* × *morifolium* (Ramat.) Hemsl. cultivars, i.e. 'UBG' and 'UPG', were used in the experiment. Single node shoot segments were used as explants. Four explants were vertically placed in the medium, per each culture jar, and treated with zinc oxide SMPs suspension (ZnO SMPs) or with NPs suspensions: ZnO NPs (1.5% H_2O), ZnO NPs (6% H_2O), ZnO + 0.1% Ag NPs (1.5% H_2O), ZnO + 0.1% Ag NPs (6% H_2O), ZnO + 1% Ag NPs (1.5% H_2O) and ZnO + 1% Ag NPs (6% H_2O) at concentrations of 100 mg · L^{-1}, 200 mg · L^{-1} or 400 mg · L^{-1}. The suspensions were sterilised in an autoclave and, before application on explants, placed for 30 min in the Elmasonic S80(H) Ultrasonic Cleaner (37 kHz, 150 W; Elma Schmidbauer GmbH, Singen, Germany) for dispersion. The suspensions were poured onto the culture medium with an automatic pipette with a sterile tip, 2 mL per culture jar. Non-treated explants inoculated on the modified MS medium were used as the control. Each experimental object consisted of 4 jars (16 single node explants in total).

In vitro cultures were maintained for 10 successive weeks in the growth room with the following conditions: 23 ± 1°C, 16/8-h light/dark light regime and photosynthetic photon flux density of 35 μmol · m^{-2} · s^{-1} (provided by Philips TLD 36W/54 fluorescent lamps, cool daylight, Koninklijke Philips Electronics N.V., Eindhoven, The Netherlands).

Biometric and biochemical analyses of chrysanthemum plantlets

To evaluate the effect of the tested SMPs and NPs on the growth and development of plantlets, the following biometric data were collected: number of leaves, micropropagation coefficient (number of descendant single node explants that could be isolated from the developed plantlet for further subculture), shoot length (cm), shoot fresh/dry weight (FW/DW) (mg) and root system fresh/dry weight (FW/DW) (mg). For the determination of shoot and root DW, the plant material was pre-dried at room temperature and then desiccated at 105˚C for 180 min in a laboratory drier (SML 42/AM, ZALMED, Warsaw, Poland) to obtain a constant dry matter.

Excised leaves and root systems were scanned with an Epson Perfection V800 scanner (Suwa, Japan). The obtained pictures were analysed to measure the leaf area (cm^2), leaf perimeter (cm), maximal leaf vertical length (cm) and maximal leaf horizontal width (cm) using the imaging software WinFOLIA™ (Reagen Instruments, Quebec, Canada), as well as the total length of the root system (cm), root system area (cm^2), root system volume (mm^3), number of root tips and number of root forks with the imaging software WinRHIZO™ (Reagen Instruments, Quebec, Canada).

The whole leaves were used as fresh tissue samples for the biochemical assay. Chlorophylls and carotenoids were extracted using 100 mg samples and 100% acetone (Chemia, Bydgoszcz, Poland) according to Lichtenthaler's (1987) procedure. The spectrophotometric analyses were performed using a NanoPhotometer® NP80 (Implen, München, Germany) at specific wavelengths (λ_{max}): for chlorophylls *a* and *b* at 645 nm and 662 nm, respectively, and for carotenoids at 470 nm. The content of the plant pigments was calculated in mg per 1 g of sample fresh weight (mg · g^{-1} FW).

Genetic stability analysis of chrysanthemum plantlets

The genetic fidelity of SMPs/NPs-treated plantlets was assessed using RAPD (Williams et al., 1990) and SCoT (Collard and Mackill, 2009) marker systems. A total of 32 'UBG'/'UPG' plantlets were included in the analysis (four from each SMPs/NPs treatment at the highest tested concentration of 400 mg · L^{-1} and four controls).

Total genomic DNA was extracted from fresh leaf tissue (100 mg) samples. The Genomic Mini AX Plant SPIN Kit (A&A Biotechnology, Gdańsk, Poland) reagents and materials were used for DNA isolation. The DNA concentration was measured using a NanoPhotometer® NP80 (Implen, München, Germany). The DNA was stored at 4˚C in Tris-EDTA (TE) buffer for a few days before the PCR.

The DNA samples were used as a template for the PCR analysis with a total of 10 primers (5 RAPD and 5 SCoT; Genomed S.A., Warsaw, Poland). PCR was performed using a BioRad C1000 Touch thermal cycler with a heated cover (Bio-Rad, Hercules, CA, USA) in

the 25-µL reaction solution. Each reaction contained 2 mM $MgCl_2$ in the reaction buffer, 1 mM dNTP solution mix, 0.05 U · µL^{-1} Taq DNA polymerase (PCR Master MixPlus, A&A Biotechnology, Gdańsk, Poland), 1 µM single primer, 0.8 ng · µL^{-1} template DNA (20 ng) and molecular water to volume. For the RAPD analysis, the following profile was applied: one cycle of 4 min at 94°C for initial DNA denaturation; 40 cycles of 1 min at 94°C for denaturation, 40 s at 42°C for annealing and 2 min at 72°C for DNA extension. The last cycle was followed by a final extension step of 4 min at 72°C. SCoT amplification was programmed as follows: one cycle of 4 min at 94°C for initial DNA denaturation; 35 cycles of 1 min at 94°C for denaturation, 50 s at 44°C for annealing and 2 min at 72°C for DNA extension. The last cycle was followed by a final extension step of 8 min at 72°C.

The PCR products were visualised on a ultraviolet (UV) light transilluminator (GelDoc XR + Gel Photodocumentation System with Image Lab 4.1 software, Bio-Rad, Hercules, CA, USA) after staining with ethidium bromide. The Gene Ruler™ Express DNA Ladder (Thermo Fisher Scientific, Waltham, MA, USA), 100–5000 bp DNA marker, was used as a size reference.

The banding patterns were scored with GelAnalyzer 23.1 software and then checked manually. For every 10 primers tested, the banding patterns were recorded as binary matrices, where '1/0' indicates the presence/absence, respectively, of a given fragment. The numbers of monomorphic (mono), polymorphic (poly) (present in the electrophoretic profile of more than one individual) and specific (spec) (unique; present in the electrophoretic profile of a single individual) *loci* were counted.

Statistical analysis

The experiment was set up in a completely randomised design. The obtained data were presented as mean ± standard deviation (SD) and subjected to one-way analysis of variance (ANOVA) and *post hoc* Fisher's test at the significance level of $p \leq 0.05$. All statistical analyses were performed with Statistica 13.3 software (StatSoft Polska, Cracow, Poland). The biometric measurements were taken from eight developed plantlets from each experimental object. For the biochemical analyses, tissue samples were collected from six plantlets from each experimental object.

RESULTS

Biometric parameters of chrysanthemum plantlets

The obtained plantlets were of high quality, with a fully developed stem, leaves and root system. No growth or physiological disorders were observed. The used material samples significantly stimulated the growth and development of plantlets in the two tested chrysanthemum cultivars. Control explants produced plantlets that were characterised by the lowest biometric parameters such as the number of leaves, micropropagation coefficient, shoot length and shoot and root system FW/DW as compared to the explants treated with all tested material samples at the whole range of applied concentrations (Figure 1, Supplementary Figure S3 and Table 1 and Table 2).

As for the 'UBG' cultivar, the highest number of formed leaves (28.75) and the highest micropropagation coefficient (26) were found for 100 mg · L^{-1} ZnO NPs (6% H_2O), whereas the values of these traits for the control amounted to 14.75 and 12, respectively. The highest values of shoot length (10.25 cm) and shoot FW (1,002.95 mg) were reported for 400 mg · L^{-1} ZnO SMPs treatment. Shoots produced on the medium with 100 mg · L^{-1} ZnO SMPs had the highest DW (122.80 mg). Material samples with Ag NPs caused a significant increase in the root system FW (129.20–146.67 mg) and DW (8.15–9.20 mg), especially treatments with 400 mg · L^{-1} ZnO + 0.1% Ag NPs (6% H_2O), 200 mg · L^{-1} ZnO + 1% Ag NPs (1.5% H_2O) and 200 mg · L^{-1} ZnO + 1% Ag NPs (6% H_2O). Contrarily, the FW/DW of the control root system amounted to 14.85/1.12 mg, respectively (Table 1).

In the 'UPG' cultivar, the development of plantlets was significantly stimulated by the treatment with 200 mg · L^{-1} ZnO + 0.1% Ag NPs (6% H_2O), which yielded the highest number of leaves (22.25), the highest micropropagation coefficient (19.50), a high shoot DW (99.28 mg) and the highest root system DW (12.98 mg). Distinctive values of biometric parameters were also found for 200 mg · L^{-1} ZnO + 1% Ag NPs (6% H_2O) application (the highest shoot length – 9.72 cm, shoot FW – 946.78 mg and shoot DW – 406.50 mg) (Table 2).

Leaf and root system architecture parameters of chrysanthemum plantlets

The detailed analysis of the leaf architecture in the two studied chrysanthemum cultivars showed that the control plantlets developed leaves with the lowest area, perimeter and width; however, no differences were found for the leaf length depending on the experimental treatments (Figure 2 and Figure 3). The application of ZnO + 0.1% Ag NPs (6% H_2O) sample at the concentration of 100 mg · L^{-1} caused a significant increase in the leaf architecture parameters in chrysanthemum 'UBG'. High values of the leaf area, perimeter and width were also reported in both cultivars for the treatment with 400 mg · L^{-1} ZnO + 1% Ag NPs (6% H_2O). However, plantlets from this experimental object did not develop as many leaves as the plantlets from the most efficient treatments in terms of the number of leaves (Table 1 and Table 2).

Supplementation with ZnO SMPs/ZnO NPs/ZnO + Ag NPs significantly improved the growth and development of the root system in 'UBG' (Figure 4).



Figure 1. Sample pictures of *Chrysanthemum* × *morifolium* 'UBG' (A) and 'UPG' (B) shoot and root systems (C, D) developed from node explants cultured *in vitro* for 10 weeks on the modified MS medium, depending on the ZnO SMPs/ZnO NPs/ZnO + Ag NPs treatment; bar = 1 cm. MS, Murashige and Skoog; NPs, nanoparticles; SMPs, submicron particles; UBG, 'UTP Burgundy Gold'; UPG, 'UTP Pinky Gold'.

The most efficient treatment in terms of the analysed parameters of the root system architecture was 200 mg · L^{-1} ZnO + 1% Ag NPs (6% H_2O). High values of the root system total length, area, volume and number of root tips and forks were also reported for other samples, i.e. 400 mg · L^{-1} ZnO + 0.1% Ag NPs (1.5% H_2O), 200 mg · L^{-1} ZnO + 0.1% Ag NPs (6% H_2O), 100 mg · L^{-1} ZnO + 1% Ag NPs (1.5% H_2O) and 400 mg · L^{-1} ZnO + 1% Ag NPs (6% H_2O). Generally, the ZnO SMPs and ZnO NPs samples less effectively stimulated the development of chrysanthemum root systems; nevertheless, the least developed roots were found in control plantlets.

On the contrary, in 'UPG', different effects of the tested material samples on the root system architecture were reported. Moreover, the obtained results were more uniform between each experimental object (Figure 5). Explants treated, both with ZnO + 1% Ag NPs (1.5% H_2O) and ZnO + 1% Ag NPs (6% H_2O) at the concentration of 200 mg · L^{-1}, formed plantlets with root systems that were characterised by the highest total length and area. Intermediate values of these traits were found in the control root system, whereas the lowest value was in the 400 mg · L^{-1} ZnO + 0.1% Ag NPs (1.5% H_2O) treatment. No significant differences between the tested experimental objects were found for the root system volume, with values ranging from 75.75 mm^3 to 122.62 mm^3. Interestingly, the highest number of root tips (46 and 45.71) was reported for the control object and 200 mg · L^{-1} ZnO + 1% Ag NPs (6% H_2O), respectively. The control object also formed the highest number of root forks (174).

Biochemical profile of chrysanthemum plantlets

In 'UBG', the highest contents of chlorophyll *a* (1.20 mg · g^{-1} FW), chlorophyll *b* (0.46 mg · g^{-1} FW), total chlorophylls (1.66 mg · g^{-1} FW) and carotenoids (0.26 mg · g^{-1} FW) were reported for 400 mg · L^{-1}

Table 1. Biometric parameters of *Chrysanthemum* × *morifolium* 'UBG' plantlets developed from node explants cultured *in vitro* on the modified MS medium, depending on the ZnO SMPs/ZnO NPs/ZnO + Ag NPs treatment.

Treatment	Number of leaves	Micropropagation coefficient	Shoot length (cm)	Shoot FW (mg)	Shoot DW (mg)	Root system FW (mg)	Root system DW (mg)
Control	14.75 ± 0.50 h	12.00 ± 0.82 i	5.20 ± 0.70 g	318.52 ± 128.04 d	34.10 ± 12.39 e	14.85 ± 9.12 c	1.12 ± 0.48 g
100 mg · L^{-1} ZnO SMPs	24.25 ± 1.89 b–e	21.50 ± 1.73 b–f	9.60 ± 1.70 ab	916.72 ± 390.89 a–c	122.80 ± 53.97 a	94.80 ± 58.17 ab	7.48 ± 3.97 a–d
200 mg · L^{-1} ZnO SMPs	22.50 ± 1.00 b–f	19.75 ± 0.96 c–h	9.00 ± 1.93 a–c	868.42 ± 338.87 a–c	91.75 ± 44.85 a–e	94.12 ± 44.37 ab	7.00 ± 3.13 a–e
400 mg · L^{-1} ZnO SMPs	25.25 ± 2.87 a–d	22.25 ± 2.87 b–e	10.25 ± 1.95 a	1,002.95 ± 389.36 a	120.58 ± 52.61 ab	107.10 ± 74.91 ab	8.00 ± 2.98 a–c
100 mg · L^{-1} ZnO NPs (1.5% H_2O)	22.50 ± 1.73 b–f	20.00 ± 1.41 c–h	8.40 ± 1.77 a–d	531.70 ± 149.45 a–d	61.52 ± 21.16 b–e	44.08 ± 27.16 ab	2.32 ± 1.38 fg
200 mg · L^{-1} ZnO NPs (1.5% H_2O)	18.50 ± 3.79 gh	16.50 ± 3.11 h	6.80 ± 1.35 c–g	598.95 ± 136.25 a–d	57.32 ± 12.32 c–e	90.28 ± 49.57 ab	4.62 ± 2.33 b–g
400 mg · L^{-1} ZnO NPs (1.5% H_2O)	19.25 ± 0.96 fg	16.50 ± 1.29 h	5.32 ± 0.64 fg	467.12 ± 222.54 cd	47.28 ± 17.01 de	52.85 ± 21.40 ab	2.98 ± 1.61 e–g
100 mg · L^{-1} ZnO NPs (6% H_2O)	28.75 ± 2.75 a	26.00 ± 2.58 a	8.62 ± 1.68 a–d	885.00 ± 378.42 a–c	104.15 ± 61.28 a–d	54.20 ± 21.37 ab	4.18 ± 2.82 b–g
200 mg · L^{-1} ZnO NPs (6% H_2O)	22.00 ± 0.82 c–g	20.00 ± 0.82 c–h	6.40 ± 1.75 d–g	594.45 ± 214.63 a–d	59.82 ± 22.95 c–e	66.62 ± 27.71 ab	3.38 ± 1.23 d–g
400 mg · L^{-1} ZnO NPs (6% H_2O)	25.75 ± 4.57 a–c	23.25 ± 4.03 a–c	7.48 ± 2.09 b–f	886.85 ± 525.24 a–c	99.62 ± 56.87 a–d	133.65 ± 79.22 a	7.25 ± 3.57 a–e
100 mg · L^{-1} ZnO + 0.1% Ag NPs (1.5% H_2O)	26.00 ± 3.92 ab	24.00 ± 3.92 ab	8.98 ± 2.35 a–c	848.98 ± 418.51 a–c	107.55 ± 60.71 a–c	71.10 ± 29.22 ab	6.35 ± 2.15 a–f
200 mg · L^{-1} ZnO + 0.1% Ag NPs (1.5% H_2O)	24.75 ± 3.30 b–e	22.50 ± 3.11 a–e	8.00 ± 1.06 a–d	699.28 ± 299.83 a–d	88.62 ± 39.66 a–e	61.50 ± 35.19 ab	4.88 ± 2.64 a–g
400 mg · L^{-1} ZnO + 0.1% Ag NPs (1.5% H_2O)	19.50 ± 2.38 fg	17.00 ± 2.58 gh	5.25 ± 1.44 e–g	503.45 ± 253.84 b–d	60.68 ± 24.29 c–e	98.58 ± 52.69 ab	4.70 ± 2.21 b–g
100 mg · L^{-1} ZnO + 0.1% Ag NPs (6% H_2O)	21.50 ± 3.70 d–g	19.50 ± 3.70 d–h	8.28 ± 2.21 a–d	822.58 ± 629.57 a–c	94.30 ± 61.92 a–d	48.22 ± 24.81 ab	2.55 ± 1.37 fg
200 mg · L^{-1} ZnO + 0.1% Ag NPs (6% H_2O)	22.75 ± 2.22 b–f	20.25 ± 2.50 c–g	9.40 ± 1.15 ab	699.20 ± 213.92 a–d	73.52 ± 13.02 a–e	78.00 ± 31.07 ab	4.52 ± 2.71 b–g
400 mg · L^{-1} ZnO + 0.1% Ag NPs (6% H_2O)	22.75 ± 2.36 b–f	20.25 ± 2.63 c–g	8.40 ± 1.87 a–d	798.75 ± 459.66 a–d	86.70 ± 35.42 a–e	146.67 ± 131.02 a	8.32 ± 2.11 ab
100 mg · L^{-1} ZnO + 1% Ag NPs (1.5% H_2O)	21.25 ± 2.22 e–g	18.75 ± 1.71 e–h	9.38 ± 0.95 ab	849.22 ± 322.33 a–c	96.32 ± 35.65 a–d	67.18 ± 33.93 ab	3.78 ± 1.60 c–g
200 mg · L^{-1} ZnO + 1% Ag NPs (1.5% H_2O)	21.50 ± 2.08 d–g	18.75 ± 2.50 e–h	7.88 ± 0.83 b–d	643.65 ± 229.90 a–d	68.72 ± 19.61 a–e	129.20 ± 53.27 a	8.15 ± 2.53 ab
400 mg · L^{-1} ZnO + 1% Ag NPs (1.5% H_2O)	20.00 ± 1.83 fg	18.00 ± 1.83 f–h	8.00 ± 1.01 a–d	788.32 ± 228.25 a–d	81.00 ± 26.56 a–e	105.08 ± 42.26 ab	7.10 ± 3.03 a–e
100 mg · L^{-1} ZnO + 1% Ag NPs (6% H_2O)	19.00 ± 2.94 fg	16.50 ± 2.65 h	6.58 ± 0.91 d–g	528.92 ± 268.54 a–d	49.15 ± 22.13 c–e	97.10 ± 40.77 ab	5.62 ± 1.70 a–f
200 mg · L^{-1} ZnO + 1% Ag NPs (6% H_2O)	21.50 ± 4.36 d–g	19.00 ± 4.08 d–h	9.58 ± 2.00 ab	987.92 ± 370.32 ab	99.85 ± 38.98 a–d	143.60 ± 45.49 a	9.20 ± 3.23 a
400 mg · L^{-1} ZnO + 1% Ag NPs (6% H_2O)	19.50 ± 2.65 fg	17.25 ± 2.22 gh	7.60 ± 1.88 b–e	724.85 ± 535.35 a–d	71.80 ± 45.90 a–e	62.32 ± 31.34 ab	4.33 ± 3.57 b–g

Means ± SD in columns followed by the same letter do not differ significantly at $p \leq 0.05$ (Fisher's test).
DW, dry weight; FW, fresh weight; MS, Murashige and Skoog; NPs, nanoparticles; SD, standard deviation; SMPs, submicron particles; 'UBG, UTP Burgundy Gold'.

Table 2. Biometric parameters of *Chrysanthemum* × *morifolium* 'UPG' plantlets developed from node explants cultured *in vitro* on the modified MS medium, depending on the ZnO SMPs/ZnO NPs/ZnO + Ag NPs treatment.

Treatment	Number of leaves	Micropropagation coefficient	Shoot length (cm)	Shoot FW (mg)	Shoot DW (mg)	Root system FW (mg)	Root system DW (mg)
Control	14.75 ± 1.50 e	11.75 ± 1.50 f	3.37 ± 0.97 e	183.88 ± 101.51 c	30.15 ± 9.71 b	14.22 ± 3.42 c	1.82 ± 1.44 d
100 mg · L^{-1} ZnO SMPs	18.50 ± 1.00 b–d	15.50 ± 1.00 c–e	8.42 ± 1.69 a–d	621.52 ± 246.24 a–c	76.82 ± 21.71 ab	97.58 ± 43.42 b	6.90 ± 4.00 bd
200 mg · L^{-1} ZnO SMPs	17.75 ± 0.96 cd	14.75 ± 0.96 e	6.55 ± 2.38 cd	525.30 ± 281.34 a–c	59.50 ± 25.42 ab	130.28 ± 45.46 b	5.28 ± 2.97 cd
400 mg · L^{-1} ZnO SMPs	19.75 ± 1.50 a–d	16.75 ± 1.50 b–e	6.85 ± 0.47 cd	610.65 ± 54.16 a–c	68.82 ± 9.47 ab	219.28 ± 82.43 b	9.15 ± 4.19 a–c
100 mg · L^{-1} ZnO NPs (1.5% H_2O)	18.75 ± 0.96 b–d	15.75 ± 0.96 c–e	6.50 ± 2.43 cd	479.82 ± 182.32 bc	58.68 ± 21.99 ab	102.65 ± 66.78 b	5.08 ± 1.42 cd
200 mg · L^{-1} ZnO NPs (1.5% H_2O)	19.00 ± 0.82 b–d	17.75 ± 2.36 a–c	7.12 ± 1.66 b–d	508.12 ± 195.29 a–c	67.40 ± 25.50 ab	122.02 ± 50.14 b	6.72 ± 2.26 cd
400 mg · L^{-1} ZnO NPs (1.5% H_2O)	20.25 ± 2.50 a–c	17.25 ± 2.50 a–e	7.58 ± 2.88 a–d	665.65 ± 271.19 ab	82.82 ± 29.18 ab	91.95 ± 53.37 b	6.08 ± 3.47 cd
100 mg · L^{-1} ZnO NPs (6% H_2O)	19.00 ± 1.41 b–d	16.00 ± 1.41 c–e	6.30 ± 1.89 de	543.68 ± 247.53 a–c	60.38 ± 26.87 ab	161.10 ± 77.52 b	7.35 ± 5.83 a–d
200 mg · L^{-1} ZnO NPs (6% H_2O)	19.75 ± 0.96 a–d	16.75 ± 0.96 b–e	7.85 ± 0.79 a–d	665.58 ± 207.59 ab	84.38 ± 32.54 ab	168.35 ± 46.40 b	7.92 ± 2.66 a–c
400 mg · L^{-1} ZnO NPs (6% H_2O)	18.50 ± 1.29 b–d	15.50 ± 1.29 c–e	6.42 ± 1.50 cd	511.45 ± 164.74 a–c	51.02 ± 14.96 ab	184.92 ± 81.48 b	6.95 ± 4.82 bd
100 mg · L^{-1} ZnO + 0.1% Ag NPs (1.5% H_2O)	20.50 ± 0.58 ab	17.75 ± 0.96 a–c	7.28 ± 1.22 a–d	753.18 ± 305.43 ab	74.85 ± 36.24 ab	101.58 ± 50.87 b	5.98 ± 2.69 cd
200 mg · L^{-1} ZnO + 0.1% Ag NPs (1.5% H_2O)	18.75 ± 0.50 b–d	15.75 ± 0.50 c–e	6.82 ± 1.25 cd	545.70 ± 131.47 a–c	61.08 ± 15.74 ab	229.28 ± 86.24 b	9.90 ± 4.08 a–c
400 mg · L^{-1} ZnO + 0.1% Ag NPs (1.5% H_2O)	19.75 ± 0.96 a–d	16.75 ± 0.96 b–e	7.08 ± 1.28 bd	678.05 ± 265.25 ab	77.95 ± 26.21 ab	186.42 ± 75.81 b	9.85 ± 4.45 a–c
100 mg · L^{-1} ZnO + 0.1% Ag NPs (6% H_2O)	20.50 ± 1.00 ab	17.50 ± 1.00 a–d	8.75 ± 1.13 a–d	755.55 ± 350.31 ab	85.68 ± 32.51 ab	140.40 ± 49.83 b	7.80 ± 3.77 a–c
200 mg · L^{-1} ZnO + 0.1% Ag NPs (6% H_2O)	22.25 ± 1.89 a	19.50 ± 1.73 a	8.82 ± 1.08 a–c	858.52 ± 283.60 ab	99.28 ± 38.17 a	210.38 ± 64.28 b	12.98 ± 1.17 a
400 mg · L^{-1} ZnO + 0.1% Ag NPs (6% H_2O)	20.75 ± 2.63 ab	17.75 ± 2.63 a–c	8.82 ± 1.11 a–c	746.30 ± 342.36 ab	83.68 ± 35.37 ab	482.35 ± 145.86 a	9.35 ± 4.15 a–c
100 mg · L^{-1} ZnO + 1% Ag NPs (1.5% H_2O)	19.50 ± 3.11 b–d	17.25 ± 3.20 a–e	8.75 ± 1.37 a–d	618.72 ± 238.85 a–c	86.40 ± 39.95 ab	135.98 ± 69.05 b	8.22 ± 2.35 a–c
200 mg · L^{-1} ZnO + 1% Ag NPs (1.5% H_2O)	18.50 ± 1.29 b–d	15.75 ± 0.96 c–e	8.80 ± 1.70 a–c	691.82 ± 299.58 ab	77.88 ± 37.48 ab	150.38 ± 58.97 b	8.92 ± 1.29 a–c
400 mg · L^{-1} ZnO + 1% Ag NPs (1.5% H_2O)	19.00 ± 1.41 b–d	16.50 ± 1.00 b–e	9.48 ± 2.30 ab	764.60 ± 356.38 ab	78.62 ± 34.05 ab	137.82 ± 37.44 b	7.92 ± 1.30 a–c
100 mg · L^{-1} ZnO + 1% Ag NPs (6% H_2O)	19.25 ± 3.77 b–d	17.25 ± 3.77 a–e	8.68 ± 3.04 a–d	687.50 ± 265.24 ab	81.50 ± 36.31 ab	104.40 ± 51.14 b	5.95 ± 5.35 cd
200 mg · L^{-1} ZnO + 1% Ag NPs (6% H_2O)	20.50 ± 1.91 ab	18.75 ± 1.50 ab	9.72 ± 1.32 a	946.78 ± 134.07 a	406.50 ± 21.20 a	231.98 ± 133.63 b	12.62 ± 3.99 ab
400 mg · L^{-1} ZnO + 1% Ag NPs (6% H_2O)	17.25 ± 2.99 de	15.00 ± 2.58 de	7.05 ± 2.36 b–d	733.92 ± 454.71 ab	74.20 ± 36.72 ab	146.40 ± 62.51 b	9.75 ± 4.49 a–c

Means ± SD in columns followed by the same letter do not differ significantly at $p \leq 0.05$ (Fisher's test).
DW, dry weight; FW, fresh weight; MS, Murashige and Skoog; NPs, nanoparticles; SD, standard deviation; SMPs, submicron particles; UPG, 'UTP Pinky Gold'.

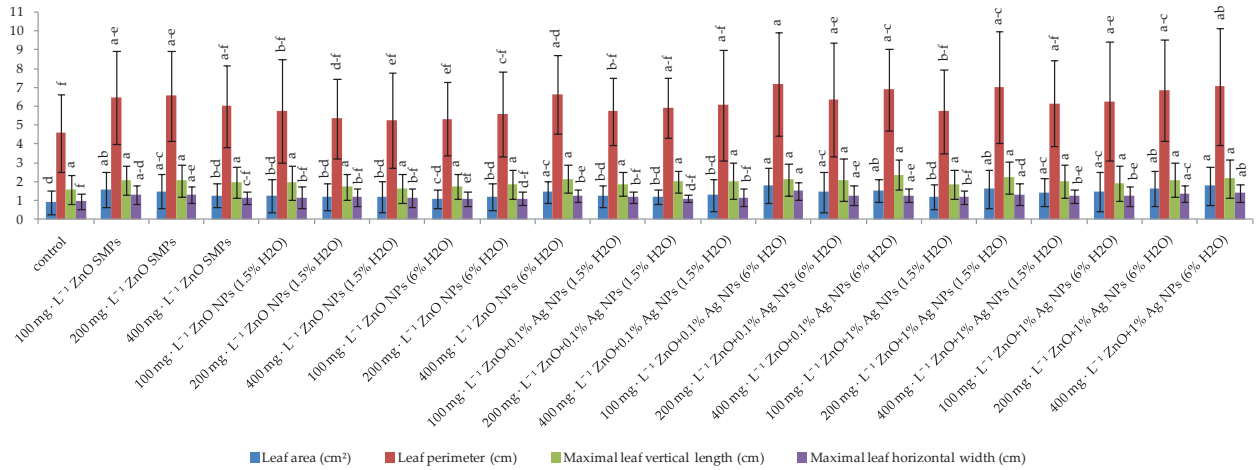


Figure 2. Leaf architecture parameters of *Chrysanthemum* × *morifolium* 'UBG' plantlets developed from node explants cultured *in vitro* on the modified MS medium, depending on the ZnO SMPs/ZnO NPs/ZnO + Ag NPs treatment. Means ± SD on graphs for each parameter analysed followed by the same letter do not differ significantly at $p \leq 0.05$ (Fisher's test). MS, Murashige and Skoog; NPs, nanoparticles; SD, standard deviation; SMPs, submicron particles; UBG, 'UTP Burgundy Gold'.

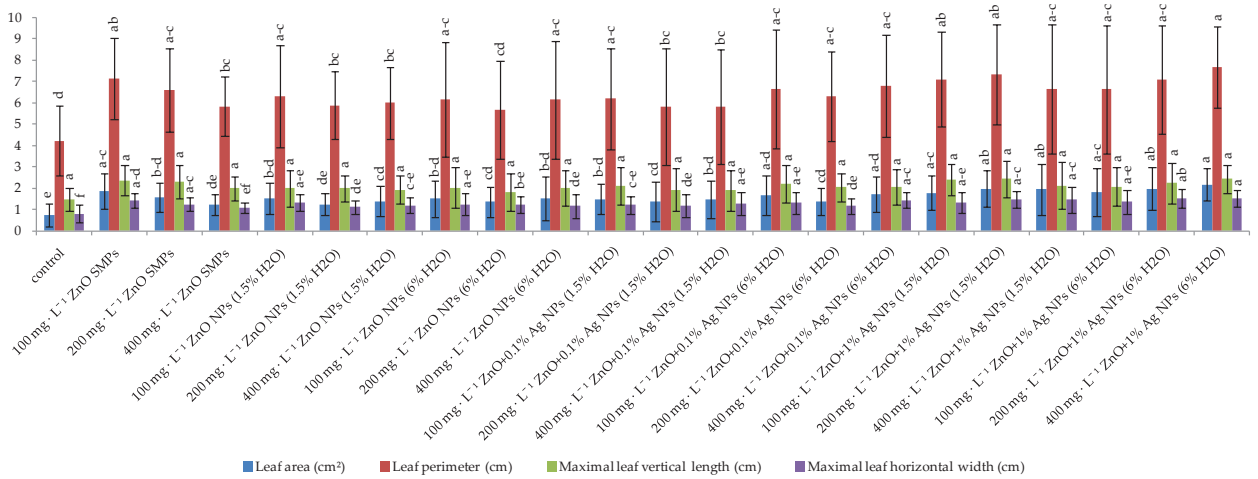


Figure 3. Leaf architecture parameters of *Chrysanthemum* × *morifolium* 'UPG' plantlets developed from node explants cultured *in vitro* on the modified MS medium, depending on the ZnO SMPs/ZnO NPs/ZnO + Ag NPs treatment. Means ± SD on graphs for each parameter analysed followed by the same letter do not differ significantly at $p \leq 0.05$ (Fisher's test). MS, Murashige and Skoog; NPs, nanoparticles; SD, standard deviation; SMPs, submicron particles; UPG, 'UTP Pinky Gold'.

ZnO NPs (1.5% H_2O) treatment. A high content of these metabolites was also found in the control, 100 mg · L^{-1} ZnO SMPs and 200 mg · L^{-1} ZnO + 1% Ag NPs (1.5% H_2O) objects. On the contrary, in 'UPG', the most efficient treatments in terms of biochemical activity of plantlets included the control, 100 mg · L^{-1} ZnO NPs (6% H_2O), 400 mg · L^{-1} ZnO + 0.1% Ag NPs (6% H_2O) and 200 mg · L^{-1} ZnO + 1% Ag NPs (1.5% H_2O). On the other hand, in other SMPs and NPs treatments, usually a decrease in the content of these metabolites was observed compared to the control, in 'UBG' and 'UPG' cultivars. The lowest contents of chlorophyll *a*, chlorophyll *b*, total chlorophylls and carotenoids were found for 400 mg · L^{-1} ZnO + 1% Ag NPs (6% H_2O) in 'UPG' and for 200 mg · L^{-1} ZnO NPs (1.5% H_2O) in 'UBG'. The highest chlorophyll *a*-to-*b* ratios were identified for 400 mg · L^{-1} ZnO SMPs in 'UBG' (2.77) and for the control in 'UPG' (2.86). Simultaneously, the highest chlorophyll-to-carotenoid ratios (7.33–7.61) were found for 200 mg · L^{-1} ZnO NPs (1.5% H_2O) treatment, in both cultivars tested (Table 3 and Table 4).

Genetic stability analysis of chrysanthemum plantlets

A total of 5,216 scorable bands were detected by five RAPD (1,888) and five SCoT (3,328) primers in the tested 'UBG' and 'UPG' plantlets. As for the RAPD

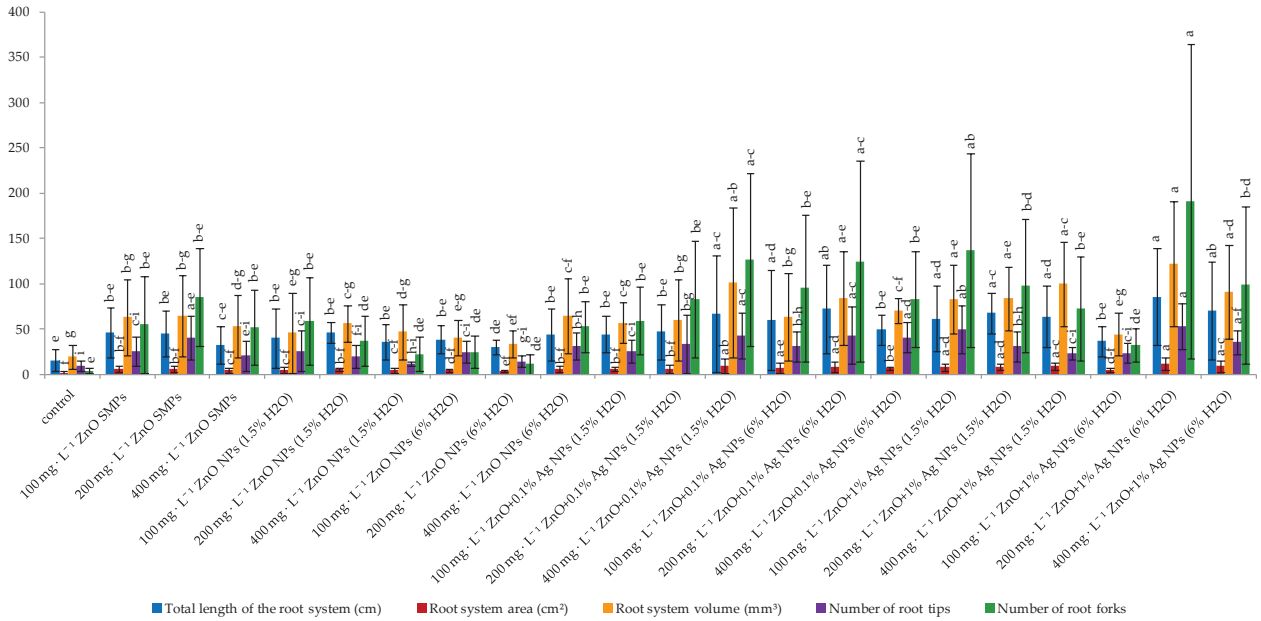


Figure 4. Root system architecture of *Chrysanthemum* × *morifolium* 'UBG' plantlets developed from node explants cultured *in vitro* on the modified MS medium, depending on the ZnO SMPs/ZnO NPs/ZnO + Ag NPs treatment. Means ± SD on graphs for each parameter analysed followed by the same letter do not differ significantly at $p \leq 0.05$ (Fisher's test). MS, Murashige and Skoog; NPs, nanoparticles; SD, standard deviation; SMPs, submicron particles; UBG, 'UTP Burgundy Gold'.

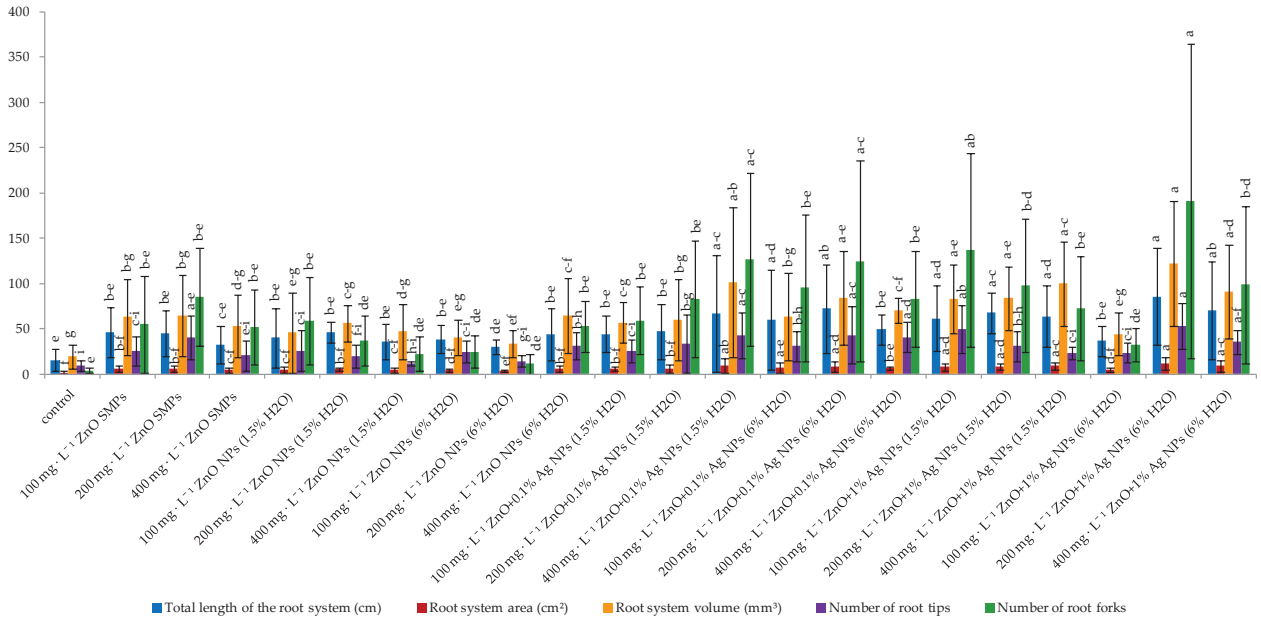


Figure 5. Root system architecture of *Chrysanthemum* × *morifolium* 'UPG' plantlets developed from node explants cultured *in vitro* on the modified MS medium, depending on the ZnO SMPs/ZnO NPs/ZnO + Ag NPs treatment. Means ± SD on graphs for each parameter analysed followed by the same letter do not differ significantly at $p \leq 0.05$ (Fisher's test). MS, Murashige and Skoog; NPs, nanoparticles; SD, standard deviation; SMPs, submicron particles; UPG, 'UTP Pinky Gold'.

marker system, primer R2 generated the highest number of bands (160 and 320 in 'UBG' and 'UPG', respectively), whereas the lowest number of bands was reported for primers R4 and R5 (160 in each cultivar). The primers R1 and R3 R2/R4 generated 5 *loci* in 'UBG' and 'UPG'. As for the SCoT marker system, primer S4 yielded the highest number of bands (832 in total) and *loci* (26 in total).

All tested RAPD and SCoT primers did not generate polymorphic products, confirming the genetic uniformity of the ZnO SMPs/ZnO NPs/ZnO + Ag NPs-treated plantlets as compared to the control within each

Table 3. Content and ratios of chlorophylls and carotenoids in *Chrysanthemum* × *morifolium* 'UBG' plantlets developed from node explants cultured *in vitro* on the modified MS medium, depending on the ZnO SMPs/ZnO NPs/ZnO + Ag NPs treatment.

Treatment	Chlorophyll *a* content (mg · g^{-1} FW)	Chlorophyll *b* content (mg · g^{-1} FW)	Chlorophyll *a*/*b* ratio	Chlorophyll (*a* + *b*) content (mg · g^{-1} FW)	Carotenoid content (mg · g^{-1} FW)	Chlorophyll/ carotenoid ratio
Control	1.13 ± 0.16 ab	0.43 ± 0.07 a–d	2.63 ± 0.05 bc	1.56 ± 0.23 ab	0.25 ± 0.03 ab	6.24 ± 0.18 c–f
100 mg · L^{-1} ZnO SMPs	1.08 ± 0.25 a–c	0.44 ± 0.09 a–c	2.45 ± 0.09 e–i	1.52 ± 0.34 a–c	0.22 ± 0.06 b–e	6.91 ± 0.41 b
200 mg · L^{-1} ZnO SMPs	0.95 ± 0.15 c–g	0.39 ± 0.03 c–f	2.44 ± 0.23 f–i	1.34 ± 0.18 c–f	0.21 ± 0.02 c–f	6.38 ± 0.27 c–f
400 mg · L^{-1} ZnO SMPs	0.83 ± 0.08 g–i	0.30 ± 0.03 j	2.77 ± 0.08 a	1.13 ± 0.11 g–i	0.17 ± 0.02 gh	6.65 ± 0.25 bc
100 mg · L^{-1} ZnO NPs (1.5% H_2O)	0.83 ± 0.10 g–i	0.33 ± 0.04 g–j	2.51 ± 0.04 d–h	1.16 ± 0.14 f–i	0.17 ± 0.02 gh	6.82 ± 0.26 b
200 mg · L^{-1} ZnO NPs (1.5% H_2O)	0.63 ± 0.03 j	0.25 ± 0.02 k	2.52 ± 0.07 c–h	0.88 ± 0.05 j	0.12 ± 0.01 i	7.33 ± 0.07 a
400 mg · L^{-1} ZnO NPs (1.5% H_2O)	1.20 ± 0.06 a	0.46 ± 0.03 a	2.61 ± 0.05 b–e	1.66 ± 0.09 a	0.26 ± 0.02 a	6.38 ± 0.26 c–f
100 mg · L^{-1} ZnO NPs (6% H_2O)	0.91 ± 0.06 e–h	0.35 ± 0.02 e–i	2.60 ± 0.06 b–f	1.26 ± 0.07 d–h	0.18 ± 0.01 f–h	7.00 ± 0.06 ab
200 mg · L^{-1} ZnO NPs (6% H_2O)	0.89 ± 0.10 f–i	0.34 ± 0.03 f–j	2.62 ± 0.10 b–d	1.23 ± 0.13 e–i	0.22 ± 0.05 b–e	5.60 ± 1.66 f
400 mg · L^{-1} ZnO NPs (6% H_2O)	0.86 ± 0.07 f–i	0.32 ± 0.04 h–j	2.69 ± 0.10 a–c	1.18 ± 0.11 e–i	0.18 ± 0.02 f–h	6.56 ± 0.11 b–d
100 mg · L^{-1} ZnO + 0.1% Ag NPs (1.5% H_2O)	1.04 ± 0.03 b–d	0.40 ± 0.01 b–e	2.60 ± 0.10 b–f	1.44 ± 0.03 b–d	0.24 ± 0.02 a–c	6.00 ± 0.34 d–f
200 mg · L^{-1} ZnO + 0.1% Ag NPs (1.5% H_2O)	0.88 ± 0.17 f–i	0.36 ± 0.05 e–i	2.44 ± 0.28 f–i	1.24 ± 0.21 e–h	0.19 ± 0.03 e–h	6.53 ± 0.11 b–d
400 mg · L^{-1} ZnO + 0.1% Ag NPs (1.5% H_2O)	0.92 ± 0.11 d–h	0.38 ± 0.07 d–g	2.63 ± 0.14 bc	1.30 ± 0.18 d–g	0.22 ± 0.03 b–e	5.91 ± 0.11 ef
100 mg · L^{-1} ZnO + 0.1% Ag NPs (6% H_2O)	1.03 ± 0.07 b–e	0.40 ± 0.04 b–e	2.58 ± 0.13 b–g	1.43 ± 0.11 b–d	0.23 ± 0.01 a–d	6.22 ± 0.36 d–f
200 mg · L^{-1} ZnO + 0.1% Ag NPs (6% H_2O)	0.79 ± 0.12 h–i	0.31 ± 0.05 ij	2.55 ± 0.06 b–g	1.10 ± 0.17 hi	0.17 ± 0.03 gh	6.47 ± 0.29 b–e
400 mg · L^{-1} ZnO + 0.1% Ag NPs (6% H_2O)	0.98 ± 0.03 c–g	0.39 ± 0.02 c–f	2.72 ± 0.04 ab	1.37 ± 0.05 c–e	0.22 ± 0.02 b–e	6.23 ± 0.24 c–f
100 mg · L^{-1} ZnO + 1% Ag NPs (1.5% H_2O)	0.99 ± 0.06 c–f	0.38 ± 0.03 d–g	2.61 ± 0.10 b–e	1.37 ± 0.09 c–e	0.22 ± 0.01 b–e	6.23 ± 0.24 c–f
200 mg · L^{-1} ZnO + 1% Ag NPs (1.5% H_2O)	1.07 ± 0.06 a–c	0.45 ± 0.03 ab	2.38 ± 0.04 hi	1.52 ± 0.08 a–c	0.22 ± 0.02 b–e	6.91 ± 0.20 b
400 mg · L^{-1} ZnO + 1% Ag NPs (1.5% H_2O)	0.76 ± 0.03 ij	0.29 ± 0.02 jk	2.62 ± 0.14 b–d	1.05 ± 0.04 i	0.16 ± 0.01 h	6.56 ± 0.18 b–f
100 mg · L^{-1} ZnO + 1% Ag NPs (6% H_2O)	0.92 ± 0.23 d–h	0.36 ± 0.08 e–i	2.56 ± 0.15 b–g	1.28 ± 0.31 d–h	0.21 ± 0.06 c–f	6.10 ± 0.47 d–f
200 mg · L^{-1} ZnO + 1% Ag NPs (6% H_2O)	0.92 ± 0.08 d–h	0.38 ± 0.02 d–g	2.42 ± 0.12 g–i	1.30 ± 0.10 d–g	0.20 ± 0.02 d–g	6.50 ± 0.22 b–d
400 mg · L^{-1} ZnO + 1% Ag NPs (6% H_2O)	0.85 ± 0.15 f–i	0.37 ± 0.08 e–h	2.30 ± 0.12 i	1.22 ± 0.22 e–i	0.20 ± 0.04 d–g	6.10 ± 0.19 d–f

Means ± SD in columns followed by the same letter do not differ significantly at $p \leq 0.05$ (Fisher's test).
MS, Murashige and Skoog; NPs, nanoparticles; SD, standard deviation; SMPs, submicron particles; UBG, 'UTP Burgundy Gold'.

Table 4. Content and ratios of chlorophylls and carotenoids in *Chrysanthemum* × *morifolium* 'UPG' plantlets developed from node explants cultured *in vitro* on the modified MS medium, depending on the ZnO SMPs/ZnO NPs/ZnO + Ag NPs treatment.

Treatment	Chlorophyll *a* content (mg · g^{-1} FW)	Chlorophyll *b* content (mg · g^{-1} FW)	Chlorophyll *a*/*b* ratio	Chlorophyll (*a* + *b*) content (mg · g^{-1} FW)	Carotenoid content (mg · g^{-1} FW)	Chlorophyll/ carotenoid ratio
Control	1.46 ± 0.06 a	0.51 ± 0.02 a–c	2.86 ± 0.06 a	1.97 ± 0.08 a	0.29 ± 0.01 ab	6.79 ± 0.07 ef
100 mg · L^{-1} ZnO SMPs	1.03 ± 0.04 fg	0.42 ± 0.03 d–f	2.45 ± 0.11 d–g	1.45 ± 0.07 d–f	0.23 ± 0.01 c–f	6.30 ± 0.26 ik
200 mg · L^{-1} ZnO SMPs	1.08 ± 0.15 e–g	0.45 ± 0.05 c–f	2.40 ± 0.06 f–h	1.53 ± 0.20 c–f	0.21 ± 0.03 d–g	7.29 ± 0.48 bc
400 mg · L^{-1} ZnO SMPs	1.03 ± 0.16 fg	0.42 ± 0.08 d–f	2.45 ± 0.08 d–g	1.45 ± 0.24 d–f	0.21 ± 0.04 d–g	6.91 ± 0.12 d–f
100 mg · L^{-1} ZnO NPs (1.5% H_2O)	1.16 ± 0.19 c–f	0.47 ± 0.06 b–e	2.47 ± 0.09 c–f	1.63 ± 0.26 b–d	0.24 ± 0.04 c–e	6.79 ± 0.30 ef
200 mg · L^{-1} ZnO NPs (1.5% H_2O)	0.97 ± 0.29 g	0.40 ± 0.12 ef	2.42 ± 0.02 e–g	1.37 ± 0.42 ef	0.18 ± 0.06 g	7.61 ± 0.36 a
400 mg · L^{-1} ZnO NPs (1.5% H_2O)	1.26 ± 0.03 b–d	0.50 ± 0.03 a–c	2.52 ± 0.11 b–d	1.76 ± 0.07 a–c	0.26 ± 0.01 bc	6.77 ± 0.15 e–g
100 mg · L^{-1} ZnO NPs (6% H_2O)	1.40 ± 0.13 ab	0.53 ± 0.04 ab	2.64 ± 0.07 b	1.93 ± 0.17 a	0.30 ± 0.03 a	6.43 ± 0.29 hi
200 mg · L^{-1} ZnO NPs (6% H_2O)	1.14 ± 0.32 c–g	0.46 ± 0.09 c–e	2.48 ± 0.23 c–e	1.60 ± 0.42 bc	0.25 ± 0.07 c–d	6.40 ± 0.17 hj
400 mg · L^{-1} ZnO NPs (6% H_2O)	1.17 ± 0.20 c–f	0.45 ± 0.07 c–f	2.60 ± 0.08 bc	1.62 ± 0.26 b–d	0.24 ± 0.04 c–e	6.75 ± 0.06 e–g
100 mg · L^{-1} ZnO + 0.1% Ag NPs (1.5% H_2O)	1.19 ± 0.09 c–f	0.48 ± 0.03 a–d	2.48 ± 0.08 c–e	1.67 ± 0.12 b–d	0.24 ± 0.01 c–e	6.96 ± 0.34 de
200 mg · L^{-1} ZnO + 0.1% Ag NPs (1.5% H_2O)	1.09 ± 0.05 d–g	0.48 ± 0.01 a–d	2.27 ± 0.06 i	1.57 ± 0.06 c–f	0.24 ± 0.02 c–e	6.54 ± 0.23 e–h
400 mg · L^{-1} ZnO + 0.1% Ag NPs (1.5% H_2O)	1.16 ± 0.09 c–f	0.49 ± 0.03 a–c	2.37 ± 0.08 g–i	1.65 ± 0.11 b–d	0.22 ± 0.02 d–g	7.50 ± 0.19 ab
100 mg · L^{-1} ZnO + 0.1% Ag NPs (6% H_2O)	1.09 ± 0.18 d–g	0.46 ± 0.08 c–f	2.37 ± 0.06 g–i	1.55 ± 0.26 c–f	0.25 ± 0.04 c–d	6.20 ± 0.08 jk
200 mg · L^{-1} ZnO + 0.1% Ag NPs (6% H_2O)	1.15 ± 0.15 c–f	0.48 ± 0.05 a–d	2.40 ± 0.07 f–h	1.63 ± 0.20 b–d	0.24 ± 0.03 c–e	6.79 ± 0.04 ef
400 mg · L^{-1} ZnO + 0.1% Ag NPs (6% H_2O)	1.30 ± 0.07 a–c	0.54 ± 0.04 a	2.41 ± 0.06 e–g	1.84 ± 0.11 ab	0.26 ± 0.01 bc	7.08 ± 0.24 de
100 mg · L^{-1} ZnO + 1% Ag NPs (1.5% H_2O)	1.02 ± 0.27 fg	0.42 ± 0.12 d–f	2.43 ± 0.08 e–g	1.44 ± 0.39 d–f	0.20 ± 0.05 e–g	7.20 ± 0.32 cd
200 mg · L^{-1} ZnO + 1% Ag NPs (1.5% H_2O)	1.25 ± 0.11 b–e	0.51 ± 0.03 a–c	2.45 ± 0.15 d–g	1.76 ± 0.14 a–c	0.27 ± 0.02 a–c	6.52 ± 0.21 f–h
400 mg · L^{-1} ZnO + 1% Ag NPs (1.5% H_2O)	1.02 ± 0.12 fg	0.45 ± 0.04 c–f	2.27 ± 0.09 i	1.47 ± 0.16 d–f	0.19 ± 0.03 f–g	7.74 ± 0.27 a
100 mg · L^{-1} ZnO + 1% Ag NPs (6% H_2O)	1.03 ± 0.07 fg	0.45 ± 0.03 c–f	2.29 ± 0.09 hi	1.48 ± 0.10 d–f	0.24 ± 0.02 c–e	6.17 ± 0.10 k
200 mg · L^{-1} ZnO + 1% Ag NPs (6% H_2O)	1.11 ± 0.11 d–g	0.44 ± 0.03 c–f	2.52 ± 0.06 b–d	1.55 ± 0.14 c–f	0.24 ± 0.02 c–e	6.46 ± 0.03 gi
400 mg · L^{-1} ZnO + 1% Ag NPs (6% H_2O)	0.96 ± 0.07 g	0.39 ± 0.03 f	2.46 ± 0.02 c–g	1.35 ± 0.10 f	0.18 ± 0.01 g	7.50 ± 0.16 ab

Means ± SD in columns followed by the same letter do not differ significantly at $p \leq 0.05$ (Fisher's test).
MS, Murashige and Skoog; NPs, nanoparticles; SD, standard deviation; SMPs, submicron particles; UPG, 'UTP Pinky Gold'.

Table 5. Molecular products obtained from *Chrysanthemum* × *morifolium* 'UBG' and 'UPG' control and 400 mg · L^{-1} ZnO SMPs/ZnO NPs/ZnO + Ag NPs-treated plantlets analysed with RAPD (R 1–5) and SCoT (S 1–5) marker systems

Primer code	Primer sequence 5′ → 3′	Reference	Cultivar	No. of bands	Band sizes (bp)	No. of loci				No. of genotypes
						Total	mono	poly	spec	
RAPD										
R1	GGG AAT TCG G	Lema-Rumińska et al. (2004)	UBG	192	367–1,478	6	6	0	0	1
			UPG	192	355–1,500	6	6	0	0	1
R2	GAC CGC TTG T		UBG	160	564–1,207	5	5	0	0	1
			UPG	320	195–2,418	10	10	0	0	1
R3	GCT GCC TCA GG	Shibata et al. (1998)	UBG	192	432–2,094	6	6	0	0	1
			UPG	192	414–2,020	6	6	0	0	1
R4	TAC CCA GGA GCG	Wolf (1996)	UBG	160	500–1,807	5	5	0	0	1
			UPG	160	500–1,910	5	5	0	0	1
R5	CAA TCG CCG T		UBG	160	534–1,449	5	5	0	0	1
			UPG	160	579–1,430	5	5	0	0	1
Σ			UBG	864		27	27	0	0	1
			UPG	1,024		32	32	0	0	1
Mean from a single primer			UBG	172.8		5.4	5.4	0	0	-
			UPG	204.8		6.4	6.4	0	0	-
SCoT										
S1	CAA TGG CTA CCA CCT	Collard and Mackill (2009)	UBG	352	425–1,762	11	11	0	0	1
			UPG	416	374–1,730	13	13	0	0	1
S2	CAA TGG CTA CCA CGT		UBG	256	531–1,757	8	8	0	0	1
			UPG	256	531–1,758	8	8	0	0	1
S3	ACG ACA TGG CGA CCA ACG		UBG	352	509–1,888	11	11	0	0	1
			UPG	288	400–1,989	9	9	0	0	1
S4	ACG ACA TGG CGA CCA TCG		UBG	416	409–2,036	13	13	0	0	1
			UPG	416	409–2,037	13	13	0	0	1
S5	ACC ATG GCT ACC GTC		UBG	320	416–2,988	10	10	0	0	1
			UPG	256	329–1,824	8	8	0	0	1
Σ			UBG	1,696		53	53	0	0	1
			UPG	1,632		51	51	0	0	1
Mean from a single primer			UBG	339.2		10.6	10.6	0	0	-
			UPG	326.4		10.2	10.2	0	0	-

mono, monomorphic; NPs, nanoparticles; poly, polymorphic; RAPD, randomly amplified polymorphic DNA; SCoT, start codon targeted polymorphism; SMPs, submicron particles; spec, specific; UBG, 'UTP Burgundy Gold'; UPG, 'UTP Pinky Gold'.

tested cultivar. Simultaneously, different band profiles were generated for 'UBG' and 'UPG' chrysanthemums, indicating the genetic distinctiveness of these two cultivars (Table 5, Figures 6 and Supplementary Figure S4).

DISCUSSION

Biometric and biochemical parameters of plants treated with NPs

Zinc is an essential constituent of enzymes and cell membranes and acts as a binding domain in many proteins, i.e. structural and transcriptional regulatory proteins. This microelement plays an important role in the biosynthesis of phytohormones, chlorophyll, proteins and carbohydrates, thus modulating plant growth and development. Plants growing in zinc-deficient environments have reduced photosynthesis and nitrogen metabolism, short internodes, curly leaves and reduced flowering, fruit development and crop production. Considering the ability of plants to accumulate ZnO NPs, these NPs can be used as an effective nanofertiliser (Sohail et al., 2020; Sarkhosh et al., 2022).

Diverse effects on biometric and biochemical parameters of micropropagated plants, due to the medium supplementation with ZnO NPs, were observed in previous studies in different species. *Olea europea* L. 'Moraiolo' shoots cultivated on the media with 2 mg · L^{-1}, 6 mg · L^{-1} and 18 mg · L^{-1} ZnO NPs had

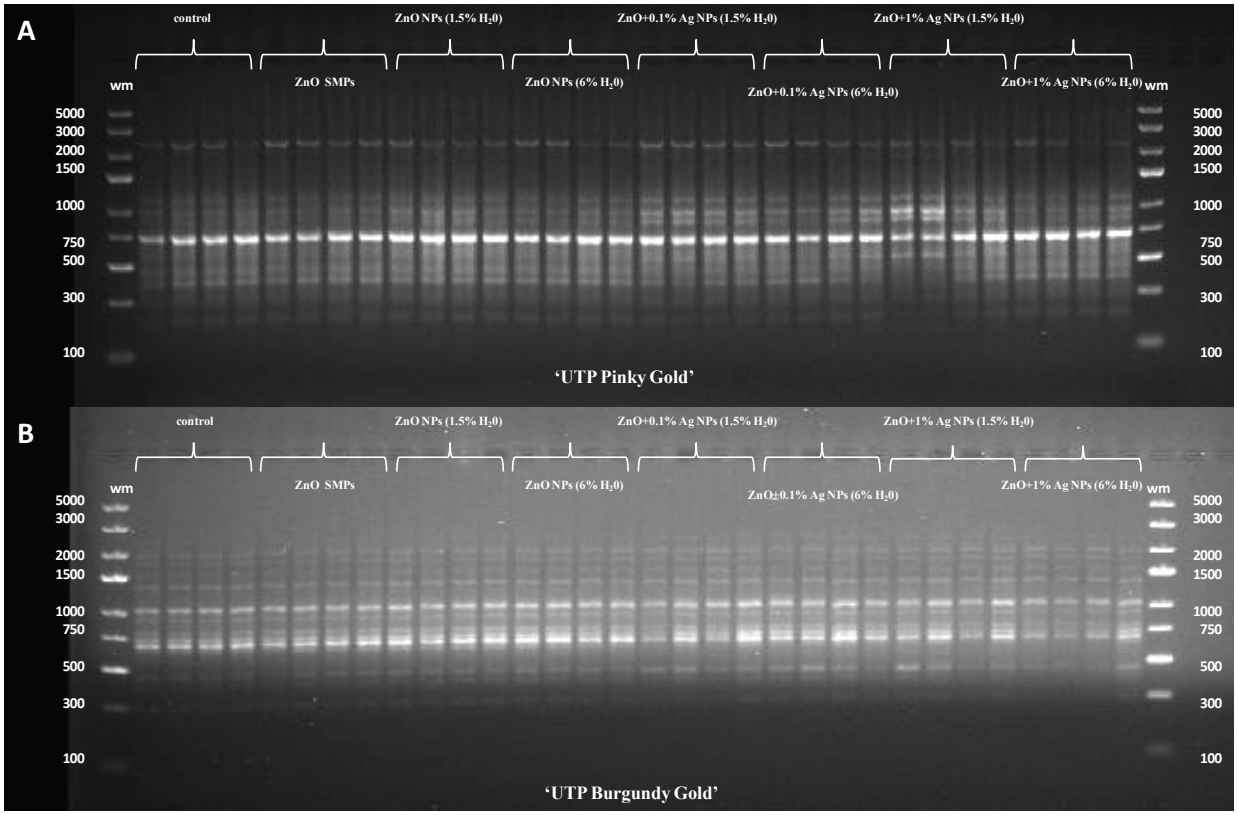


Figure 6. Example of RAPD (A) and SCoT (B) band profiles of the control and 400 mg · L^{-1} ZnO SMPs/ZnO NPs/ZnO + Ag NPs-treated plantlets of *Chrysanthemum* × *morifolium* 'UBG' and 'UPG' received as a result of electrophoresis of the DNA amplification products obtained with the R2 (RAPD) and S4 (SCoT) primers. Outermost lanes (wm) are DNA bp weight markers. NPs, nanoparticles; RAPD, randomly amplified polymorphic DNA; SCoT, start codon targeted polymorphism; SMPs, submicron particles; UBG, 'UTP Burgundy Gold'; UPG, 'UTP Pinky Gold'.

a higher number of nodes, fresh and dry weight than the control. The treatment with 6 mg · L^{-1} and 18 mg · L^{-1} ZnO NPs positively influenced the protein and chlorophyll *a* and *b* content. The results confirmed the Zn capacity for stimulating nutrient acquisition and, in turn, protein biosynthesis and biomass accumulation (Regni et al., 2021). In the study on *Punica granatum* L., the addition of ZnO NPs to the medium at low concentrations (1 mg · L^{-1}, 2.5 mg · L^{-1}, and 5 mg · L^{-1}) promoted the multiplication coefficient, shoot length, fresh and dry weight rather than higher concentrations (7.5 mg · L^{-1} and 10 mg · L^{-1}), indicating that ZnO NPs can induce different effects in plants in a dose-dependent manner. Moreover, 1 mg · L^{-1} and 2.5 mg · L^{-1} ZnO-NPs significantly improved the content of the photosynthetic pigments. However, reduction in the pigments was observed at higher concentrations (7 mg · L^{-1} and 10 mg · L^{-1}), suggesting that the appropriate amount of ZnO NPs can enhance the photosynthetic activity of plants and that Zn plays an important role in improving the biosynthesis of chlorophyll and carotenoids (El-Mahdy and Elazab, 2020). Likewise, dose-dependent effects of ZnO NPs on plant growth and phytochemical profile were reported in *in vitro* studies for *Pisum sativum* L. (Geyik et al., 2022), Solanum lycopersicum Mill. (Alharby et al., 2016), *Solanum tuberosum* L. (Alghamdi et al., 2022) and *Vigna radiata* (L.) R. Wilczek (Sorahinobar et al., 2022) and in *in vivo* studies for *Brassica oleracea* var *italica* (Awan et al., 2021), *Linum usitatissimum* L. (Sadak and Bakry, 2020), *Oryza sativa* L. (Zhang et al., 2021) or *Chrysanthemum* × *morifolium* (Oraghi Ardebili and Sharifi, 2018). Growth and photosynthesis parameters in *Triticum aestivum* L. plants developed from ZnO NPs-treated seeds increased linearly with the increasing NPs concentrations, from 25 mg · L^{-1} to 100 mg · L^{-1} (Munir et al., 2018).

Changes in the Zn status of the plant may modify its phytohormonal balance, significantly affecting the growth process (Oraghi Ardebili and Sharifi, 2018). Moreover, ZnO NPs stimulate the transfer of iron, potassium and phosphorus from roots to shoots, thus increasing the availability of these elements. This, in turn, causes an increase in carbohydrate biosynthesis in plants (Awan et al., 2021). Interestingly, the comparative transcriptomic analysis revealed that ZnO NPs can upregulate the expression of a set of genes encoding antioxidative enzymes, transporters and enzymes or regulators involved in nutrient element transport, carbon/nitrogen metabolism and secondary metabolism in plants (Sun et al., 2020). The mentioned

multifaced interactions of Zn with physiological and growth processes in plants contributed most likely to the increases in biometric parameters of the tested 'UBG' and 'UPG' plantlets and allowed to improve the efficiency of micropropagation.

The ZnO NPs-induced increase in the chlorophyll content may result from the zinc involvement in chlorophyll formation by protochlorophyllide and chloroplast development when ZnO NPs are applied at low concentrations. In contrast, high ZnO NPs concentrations, by providing excessive zinc to the plant, can inhibit chlorophyll formation by interfering with the expression of genes associated with chlorophyll biosynthesis, reduce chlorophyll fluorescence parameters and photosynthetic efficiency and in turn, lead to a reduction in biomass accumulation (Wang et al., 2018; Del Buono et al., 2021). Similarly, specific, non-excessive concentrations of ZnO NPs can stimulate carotenoid biosynthesis; however, higher concentrations interfere with the biosynthesis of these pigments. Carotenoids are not only important light-harvesting pigments in the photosynthesis process, but they have also antioxidant activity and are involved in removing reactive oxygen species (ROS), protecting chloroplasts from NPs-induced oxidative stress through their ability to quench chlorophyll in a singlet or triplet form (Del Buono et al., 2021). In the present study, as compared to the control, the SMPs- and NPs-treated chrysanthemums were characterised by a similar, or most often, lower content of chlorophylls and carotenoids; however, no visible symptoms of zinc excess or deficiency were detected. These results, on the one hand, may reflect the use of high concentrations of ZnO SMPs/NPs and their inhibiting effect on plant pigment biosynthesis, and/or induction of oxidative stress. On the other hand, the SMPs/NPs-treated plantlets presented significantly higher biometric parameters than control plantlets, and we presume that most likely, intensive-growing young plant tissues might have accumulated less pigments.

Some of the tested ZnO NPs material samples contained 0.1% or 1% Ag NPs, and we observed positive effects of silver NPs on the analysed parameters of plantlets. The results obtained by Hegazi et al. (2021) indicate that the medium supplementation with 5 mg · L^{-1} Ag NPs increased bud sprouting, shoot length, number of shoots per explant and number of leaves per shoot in *O. europea*. Similarly, *Musa* spp. shoots cultured on the medium with 1 mg · L^{-1} Ag NPs presented 8.4 times higher multiplication rate and three-fold higher total chlorophyll content than the control (Do et al., 2018).

In our study, the tested material samples highly improved the growth and development of root systems in the two studied cultivars. Similarly, significant increases in *Zea mays* L. roots in response to 1 mg · L^{-1}, 10 mg · L^{-1}, 100 mg · L^{-1} and 500 mg · L^{-1} ZnO NPs were reported (López-Reyes et al., 2022). Promising treatment for *in vitro* rooting of a difficult-to-root cultivar of *Malus domestica* Borkh. was the use of ZnO NPs loaded with indole-3-acetic acid (IAA) or indole-3-butyric acid (IBA) (Alizadeh and Dumanoğlu, 2022). Nevertheless, as the concentration of ZnO NPs increased (5–20 mg · L^{-1}), a decrease in the number of lateral roots and thickening of roots were observed in *Solanum melongena* L. (Thunugunta et al., 2018), which indicates the species specificity in response to NPs treatment. Moreover, in our study, differences in rhizogenesis were found between the two tested chrysanthemum cultivars in reaction to particular treatments.

Being an enzymatic constituent, Zn has an important function in the synthesis and accumulation of free amino acids. For example, tryptophan is a precursor of natural auxin IAA, which stimulates root formation and improves the root system architecture (Li et al., 2021; Sarkhosh et al., 2022). Pandey et al. (2010) proved that ZnO NPs gave a very positive response in root development in *Cicer arietinum* L. acting as a stimulator of IAA biosynthesis. Most likely, in our research, zinc stimulated the formation of endogenous auxins, and then, auxins induced rhizogenesis. At the same time, in our study, we observed intensive root formation and development after the use of ZnO NPs samples containing Ag NPs. Silver NPs, used at low concentrations of 3 mg · L^{-1}, stimulated the regeneration of adventitious roots in *P. dactylifera* (Elsayh et al., 2022) and *Musa* spp. (Do et al., 2018). On the contrary, in our previous study, 10 mg · L^{-1} and 30 mg · L^{-1} Ag NPs limited chrysanthemum rooting, which was in line with other scientific reports on rhizogenesis inhibition observed at higher Ag NPs concentrations (Tymoszuk and Miler, 2019).

Positive, negative or non-significant effects of various NPs on plants depend also on the NP's size and shape, the method of NPs synthesis and the solvents used for synthesis (Thunugunta et al., 2018). The physicochemical properties of NPs differ significantly from the corresponding bulk material; thus, NPs can differently affect biological processes in living cells (Thunugunta et al., 2018). Higher efficiency of ZnO NPs for enhancing growth parameters than the macro size $ZnSO_4$ salt was reported in *B. oleracea* var. *italica*. According to the authors, ZnO NPs are usually absorbed in a higher rate and with more feasibility by plants than $ZnSO_4$ in macro size and are considered to be more reactive due to their nanometric size and larger surface area as compared to their macro counterparts (Awan et al., 2021). Both macro and nano ZnO enhanced growth and yield parameters in *L. usitatissimum* L.; however, NPs were most effective at lower concentrations than macro particles (Sadak and Bakry, 2020). Likewise, a higher zinc content was accumulated in *N. tabacum* L. callus cells under ZnO NPs treatment than under ZnO microparticle treatment (Mazaheri-Tirani and Dayani, 2020). Similarly in our study, the highest values of the evaluated biometric parameters of chrysanthemum

plantlets were usually noticed when ZnO NPs were applied as compared to ZnO SMPs, suggesting that small NPs were easily absorbed and, therefore, more effective than larger SMPs.

In the present study, for samples ZnO SMPs, ZnO NPs (1.5% H_2O), ZnO NPs (6% H_2O), ZnO + 0.1% Ag NPs (1.5% H_2O), ZnO + 0.1% Ag NPs (6% H_2O), ZnO + 1% Ag NPs (1.5% H_2O) and ZnO + 1% Ag NPs (6% H_2O), the particle size was 240 nm, 25 nm, 65 nm, 29 nm, 79 nm, 27 nm and 53 nm, respectively. The best developed plantlets were obtained after the use of samples containing a higher water content and larger particle size, especially ZnO NPs (6% H_2O) (65 nm), ZnO + 0.1% Ag NPs (6% H_2O) (79 nm) and ZnO + 1% Ag NPs (6% H_2O) (53 nm), as compared to their counterparts with lower water content (1.5%) and smaller particle size (25–29 nm). It can, therefore, be concluded that smaller NPs are more toxic to plants, limiting their growth and development. Smaller NPs have a larger SSA and, thus, more available surface area to interact with cellular components such as nucleic acids, proteins, fatty acids and carbohydrates. The smaller size also likely makes it possible to enter the cell, causing cellular damage (Huang et al., 2017).

Each species responds differently to the application of ZnO NPs, either at a biometric or at a biochemical level. As was presented in the study performed by López-Reyes et al. (2022), some species are more sensitive (*Phaseolus vulgaris* L.) or more tolerant (*Z. mays* L.) to the same ZnO NPs treatment (1–500 mg · L^{-1}). Zinc submicron/nano/particles' effect on plants differs between related cultivars of the same species, which was proved in the present study, as well as in our previous experiment on adventitious organogenesis in chrysanthemum (Tymoszuk et al., 2022). Interestingly, NPs can differently affect plant growth in tissue culture conditions as compared to greenhouse conditions, as was reported for *S. melongena* L., when the ZnO NPs toxicity was higher in culture medium than in soil (Thunugunta et al., 2018). At the same time, attention should be paid to the method used for the material sample application. In previous studies, NPs were usually added directly into the *in vitro* culture medium during its preparation, whereas in our study, the tested material samples were poured, at relatively high concentrations, on the surface of the medium and inoculated explants. In this approach, particles could cover explants and penetrate the outer layer of the medium and were more available for the explants, especially during the early stage of culture. When adding NPs into the whole volume of the medium, particles most often sediment into its deepest layers during solidification and become less accessible for explants.

Considering the data obtained in this study and results reported by other authors, it can be stated that highly differentiated properties of NPs, plant species specificity, different NPs treatments and variable experimental conditions are crucial factors determining multidirectional effects of NPs on plants and highlighting possible uses of NPs in plant production. The comprehensive understanding of nanoparticle *versus* plant interactions requires further detailed studies for science and practice implementation.

Genetic stability of plants treated with NPs

RAPD and SCoT markers are rapid and reliable tools for monitoring NPs-induced genetic effects in plants, being sensitive methods capable of detecting variations in genome profiles (Plaksenkova et al., 2020). As was demonstrated in the present study, based on the RAPD and SCoT analysis, the 400 mg · L^{-1} ZnO SMPs/ZnO NPs/ZnO + Ag NPs-treated chrysanthemums were genetically stable, presenting the same genomic profiles as the control plants. Interestingly, RAPD and SCoT markers were effective in polymorphism screening in adventitious shoots regenerated from leaf explants in 50 mg · L^{-1} and 100 mg · L^{-1} Ag NPs-treated 'Lilac Wonder' and 'Richmond' chrysanthemums (Tymoszuk and Kulus, 2022). Nevertheless, there is a fundamental difference between the regeneration of adventitious shoot from the *de novo*-formed adventitious meristem on non-meristematic explants such as leaf or internodes, and the growth of axillary shoot from the preexisting axillary meristem on nodal explants. The regeneration of adventitious shoots is related to the acquisition of pluripotency by the cell and its further dedifferentiation and redifferentiation. According to the stochastic model developed by Broertjes and Keen (1980), the adventitious meristem is most often formed from a single explant cell. If this cell is genetically changed due to NPs treatment, the emerging adventitious shoot may present different RAPD or SCoT band profiles (Broertjes and van Harten, 1988; Shin et al., 2020; Tymoszuk and Kulus, 2022). Moreover, through the mechanism of selection (diplont or diplontic), genetically changed cells in deeper tissue layers of the axillary meristem are eliminated by fast-dividing and more vital non-changed cells (Broertjes and van Harten, 1988; Zalewska et al., 2011). This may explain the results obtained in the present study, confirming that chrysanthemum shoots developing from axillary meristems exposed to ZnO SMPs/ZnO NPs/ZnO + Ag NPs are genetically stable.

Excess zinc, typically >400 mg · kg^{-1} Zn in tissue dry weight, is toxic to plants. Zinc toxicity leads to several implications in many metabolic processes and can cause genetically related disorders since Zn is a constituent of proteins related to DNA and RNA stabilisation (da Cruz et al., 2019). ZnO NPs at the concentrations of 1 mg · L^{-1}, 2 mg · L^{-1} and 4 mg · L^{-1} enhanced *Hordeum vulgare* L. seeds germination, as well as shoot and root elongation; however, the RAPD analysis results proved that ZnO NPs treatment decreased genomic template stability and up-/downregulated miRNAs (Plaksenkova et al., 2020). Kumari et al. (2011) reported cytogenetic and genotoxic effects of ZnO NPs on the root cells of *Allium cepa* L., namely, with the increasing concentrations of

ZnO NPs (25 mg · L^{-1}, 50 mg · L^{-1}, 75 mg · L^{-1}, and 100 mg · L^{-1}), the mitotic index decreased with the increase in pycnotic cells, while micronuclei index and chromosomal aberration index increased. Similarly, in the root meristem cells of *A. cepa* treated with 200 mg · L^{-1}, 400 mg · L^{-1} and 800 mg · L^{-1} ZnO NPs, increased chromosome aberrations, micronucleus formation, DNA strand breaks and cell cycle arrest at the G2/M checkpoint were observed by Ghosh et al. (2016). ZnO NPs, CuO NPs and γ-Fe_3O_4 increased the polymorphism rate and cytosine methylation while reducing genomic template stability in the *in vitro* culture of *T. aestivum* L. mature embryos. However, the consequences of these changes have not been fully elucidated (Haliloğlu et al., 2022). Interestingly, ZnO NPs induced oxidative stress and DNA damage in *Lathyrus sativus* L., but to a lesser extent than cationic Zn^{2+} from $Zn(CH_3COO)_2$ (Panda et al., 2017). Nevertheless, plants have some homeostatic defence mechanisms, which can be activated before the appearance of toxicity symptoms. The altered Zn levels activate genes to avoid excessive or poor absorption and accumulation in plant tissues such as transcriptional factors, enzymes, channels and transporters (da Cruz et al., 2019). As the results of the present study indicate, the SMPs/ZnO NPs/ZnO + Ag NPs concentrations of 400 mg · L^{-1} were not genotoxic to plants, or plants have activated appropriate detoxification mechanisms. Nevertheless, these assumptions should be investigated more thoroughly by determining the zinc content in plant tissues or by examining the activity of previously mentioned genes involved in homeostatic defence mechanisms. Interestingly, Aly et al. (2023) in their recent study pointed out ZnO NPs as a potential nano-protective agent that can reduce irradiation-induced molecular variation in *Spinacia oleracea* L. plants.

Ag NPs are also known for their genotoxic properties in plants. As reported by Patlolla et al. (2012) in *Vicia faba* L. root meristem cells, Ag NPs treatment induced, in a dose-dependent manner (12.5–100 mg · L^{-1}), an increased number of structural chromosomal aberrations and micronuclei induction and decreased the value of the mitotic index. The 10 mg · L^{-1}, 20 mg · L^{-1}, 40 mg · L^{-1} and 50 mg · L^{-1} Ag NPs-treated root tip cells of *T. aestivum* L. exhibited various types of chromosomal aberrations, such as incorrect orientation at metaphase, chromosomal breakage, metaphasic plate distortion, spindle dysfunction, stickiness, aberrant movement at metaphase, fragmentation, scattering, unequal separation, scattering, chromosomal gaps, multipolar anaphase, erosion and distributed and lagging chromosomes (Abdelsalam et al., 2018). Ag NPs phytotoxicity is often the result of the overproduction of ROS, leading to oxidative stress in plant cells and, finally, DNA damage (Patlolla et al., 2012). Moreover, the cationic Ag^+ released inside plant cells from Ag NPs can interact chemically or physicochemically with nucleic acids and induce DNA disruption (Speranza et al., 2013). Nevertheless, plants can activate enzymatic and non-enzymatic defence systems to cope with the toxic effects of oxidative stress (Tripathi et al., 2016). In the present study, a decrease in the content of chlorophylls and carotenoids was most often observed in the ZnO SMPs/ZnO NPs/ZnO + Ag NPs-treated chrysanthemum as compared to the control, in both 'UBG' and 'UPG' cultivars. This may indicate, in part, the occurrence of oxidative stress resulting from the NPs application. On the other hand, the content of Ag NPs in the tested material samples was low, most likely too low, to induce genetic variation as compared to other studies on the genotoxic effects of Ag NPs.

CONCLUSIONS

Our study focused on the application of zinc oxide and silver NPs in chrysanthemum micropropagation *via* nodal culture. The obtained results provide a better understanding of the multifaceted effects of ZnO SMPs, ZnO NPs and ZnO + Ag NPs at the concentrations of 100 mg · L^{-1}, 200 mg · L^{-1} or 400 mg · L^{-1} on chrysanthemum plantlets at the biochemical, genetic and biometric levels and are of importance for modern horticulture. We revealed that tested material samples significantly improved the micropropagation efficiency and shoot/root growth parameters and influenced the biochemical stability but did not induce genetic variation in the tested cultivars. Such promising results can be implemented in large-scale commercial production of true-to-type chrysanthemum plants, as well as in breeding programmes to intensify the growth and propagation of valuable, individual genotypes. Our future studies will focus on the detailed analysis of NPs accumulation and the profile of different metabolites in chrysanthemum plants in response to ZnO NPs treatment.

ACKNOWLEDGMENTS

The authors would like to thank Ewelina Karcz, Marceli Gawroński, Jan Mizeracki and Svetlana Stelmakh for their technical support in this research study.

FUNDING

Characterisation studies of nanomaterials were conducted using equipment funded by the Center for Preclinical Research and Technology—CePT I (POIG.02.02.00-14-024/08), financed by the European Regional Development Fund 'Innovative Economy' for years 2007–2013 and CePT II (RPMA.01.01.00-14-8476/17-07) from Regional Operational Programme of the Mazowieckie Voivodeship 2014–2020.

AUTHOR CONTRIBUTIONS

A.T.: conceptualisation, methodology, validation, formal analysis, investigation, data curation, writing – original draft, writing – review and editing, visualisation,

supervision and project administration. U.S.: methodology, formal analysis and investigation. J.W.: methodology, validation, formal analysis, investigation, writing – original draft, writing – review and editing and visualisation. J.K.: formal analysis and writing – review and editing. M.A.: formal analysis and data curation. D.K.: validation, formal analysis, investigation and writing – review and editing. All authors have read and agreed to the published version of the manuscript. This report is part of A.T. habilitation thesis.

CONFLICT OF INTEREST

The authors declare no conflict of interest.

DATA AVAILABILITY

Data available by e-mail on reasonable request.

SUPPLEMENTARY MATERIALS

Supplementary Table S1. Composition of the precursor solution used for synthesis. Supplementary Table S2. Characteristics of samples. Supplementary Table S3. Results of the analysis of the chemical composition of the sample. The method of analysis was energy-dispersive spectrometry (EDS). Supplementary Figure S1. X-ray diffraction patterns of samples. Supplementary Figure S2. SEM images of samples: (a, b) ZnO SMPs; (c, d) ZnO NPs (1.5% H_2O); (e, f) ZnO NPs (6% H_2O); (g, h) ZnO + 0.1% Ag NPs (1.5% H_2O); (i, j) ZnO + 0.1% Ag NPs (6% H_2O); (k, l) ZnO + 1% Ag NPs (1.5% H_2O); (m, n) ZnO + 1% Ag NPs (6% H_2O) images taken with the immersion lens detector.

REFERENCES

Abdelsalam, N. R., Abdel-Megeed, A., Ali, H. M., Salem, M. Z. M., Al-Hayali, M. F. A., and Elshikh, M. S. (2018). Genotoxicity effects of silver nanoparticles on wheat (*Triticum aestivum* L.) root tip cells. *Ecotoxicology and Environmental Safety, 155,* 76–85, https://doi.org/10.1016/j.ecoenv.2018.02.069.

Alghamdi, E. S., Farooq, M., and Metwali, E. M. R. (2022). Influence of nano zinc oxide on the *in vitro* callus growth, *ex vitro* tuber yield and nutritional quality of potato (*Solanum tuberosum* L.) cultivars under salt stress. *Journal of Animal and Plant Sciences, 32*(2), 440–449, https://doi.org/10.36899/JAPS.2022.0441.

Alharby, H. F., Metwali, E. M. R., Fuller, M. P., and Aldhebiani, A. Y. (2016). Impact of application of zinc oxide nanoparticles on callus induction, plant regeneration, element content and antioxidant enzyme activity in tomato (Solanum lycopersicum Mill.) under salt stress. *Archives of Biological Sciences, 68*(4), 723–735, https://doi.org/10.2298/ABS151105017A.

Alizadeh, S., and Dumanoğlu, H. (2022). The effects of zinc oxide nanoparticles loaded with IAA and IBA on *in vitro* rooting of apple microcuttings. *Turkish Journal of Agriculture and Forestry, 46*, 306–317, https://doi.org/10.55730/1300-011X.3004.

Aly, A. A., Safwat, G., Eliwa, N. E., Eltawil, A. H. M., and Abd el-aziz, M. H. (2023). Changes in morphological traits, anatomical and molecular alterations caused by gamma-rays and zinc oxide nanoparticles in spinach (*Spinacia oleracea* L.) plant. *Biometals, 36*, 1059–1079, https://doi.org/10.1007/s10534-023-00505-w.

Awan, S., Shahzadi, K., Javad, S., Tariq, A., Ahmad, A., and Ilyas, S. (2021). A preliminary study of influence of zinc oxide nanoparticles on growth parameters of *Brassica oleracea* var *italica*. *Journal of the Saudi Society for Agricultural Sciences, 20*, 18–24, https://doi.org/10.1016/j.jssas.2020.10.003.

Award, K. M., Al-Mayahi, A. M. W., Mahdi, M. A., Al-Asadi, A. S. M., and Abass, M. H. (2020). *In vitro* assessment of ZnO nanoparticles on *Phoenix dactylifera* L. micropropagation. *Scientific Journal of King Faisal University (Basic and Applied Sciences), 21*(1), 1441 H, https://doi.org/10.37575/b/agr/2000.

Broertjes, C., and Keen, A. (1980). Adventitious shoots: Do they develop from one cell? *Euphytica, 29*, 73–87, https://doi.org/10.1007/BF00037251.

Broertjes, C., and Van Harten, A. A. (1988). *Applied mutation breeding for vegetatively propagated crops*. The Netherlands, Amsterdam: Elsevier.

Collard, B. C. Y., and Mackill, D. J. (2009). Start codon targeted (SCoT) polymorphism: A simple, novel DNA marker technique for generating gene-targeted markers in plants. *Plant Molecular Biology Reporter, 27*, 86–93, https://doi.org/10.1007/s11105-008-0060-5.

Da Cruz, T. N. M., Savassa, S. M., Montanha, G. S., Ishida, J. K., De Almeida, E., Tsai, S. M., Lavres Junior, J., and De Carvalho, H. W. P. (2019). A new glance on root-to-shoot *in vivo* zinc transport and time-dependent physiological effects of $ZnSO_4$ and ZnO nanoparticles on plants. *Scientific Reports, 9*, 10416, https://doi.org/10.1038/s41598-019-46796-3.

Del Buono, D., Di Michele, A., Costantino, F., Trevisan, M., and Lucini, L. (2021). Biogenic ZnO nanoparticles synthesized using a novel plant extract: Application to enhance physiological and biochemical traits in maize. *Nanomaterials, 11*, 1270, https://doi.org/10.3390/nano11051270.

Do, D. G., Dang, T. K. T., Nguyen, T. H. T., Nguyen, T. D., Tran, T. T., and Hieu, D. D. (2018). Effects of nano silver on the growth of banana (*Musa* spp.) cultured *in vitro*. *Journal of Vietnamese Environment, 10*(2), 92–98, https://doi.org/10.13141/jve.vol10.no2.pp92-98.

El-Mahdy, M. T., and Elazab, D. S. (2020). Impact of zinc oxide nanoparticles on pomegranate growth

under *in vitro* conditions. *Russian Journal of Plant Physiology, 67*, 162–167, https://doi.org/10.1134/S1021443720010045.

Elsayh, S. A. A, Arafa, R. N., Ali, G. A., Abdelaal, W. B., Sidky, R. A., and Ragab, T. I. M. (2022). Impact of silver nanoparticles on multiplication, rooting of shoots and biochemical analyses of date palm Hayani cv. by *in vitro*. *Biocatalysis and Agricultural Biotechnology, 43*, 102400, https://doi.org/10.1016/j.bcab.2022.102400.

Elshoky, H. A., Yotsova, E., Farghali, M. A., Farroh, K. Y., El-Sayed, K., Elzorkany, H. E., Rashkov, G., Dobrikova, A., Borisova, P., Stefanov, M., Ali, M. A., and Apostolova, E. (2021). Impact of foliar spray of zinc oxide nanoparticles on the photosynthesis of *Pisum sativum* L. under salt stress. *Plant Physiology and Biochemistry, 167*, 607–618, https://doi.org/10.1016/j.plaphy.2021.08.039.

García-López, J. I., Zavala-García, F., Olivares-Sáenz, E., Lira-Saldívar, R. H., Díaz Barriga-Castro, E., Ruiz-Torres, N. A., Ramos-Cortez, E., Vázquez-Alvarado, R., and Niño-Medina, G. (2018). Zinc oxide nanoparticles boost phenolic compounds and antioxidant activity of *Capsicum annuum* L. during germination. *Agronomy, 8(10)*, 215, https://doi.org/10.3390/agronomy8100215.

Geyik, M. S., Yazicilar, B., Ata, S., and Bezirganoglu, İ. (2022). *In vitro* ZnO nanoparticles enhanced pea (*Pisum sativum* L.) seedlings growth. *Turkish Journal of Agricultural and Natural Sciences, 9*(4), 1080–1087, https://doi.org/10.30910/turkjans.1115351.

Ghosh, M., Jana, A., Sinha, S., Jothiramajayam, M., Nag, A., Chakraborty, A., Mukherjee, A., and Mukherjee, A. (2016). Effects of ZnO nanoparticles in plants: Cytotoxicity, genotoxicity, deregulation of antioxidant defenses, and cell-cycle arrest. *Mutation Research: Genetic Toxicology and Environmental Mutagenesis, 807*, 25–32, https://doi.org/10.1016/j.mrgentox.2016.07.006.

Gu, J., Scotti, F., Reich, E., Kirchhof, R., Booker, A., and Heinrich, M. (2022). Chrysanthemum species used as food and medicine: Understanding quality differences on the global market. *South African Journal of Botany, 148*, 123–134, https://doi.org/10.1016/j.sajb.2022.04.009.

Haliloğlu, K., Türkoğlu, A., Balpinar, Ö., Nadaroğlu, H., Alayli, A., and Poczai, P. (2022). Effects of zinc, copper and iron oxide nanoparticles on induced DNA methylation, genomic instability and LTR retrotransposon polymorphism in wheat (*Triticum aestivum* L.). *Plants, 11*(17), 2193, https://doi.org/10.3390/plants11172193.

Hao, D.-C., Song, Y., Xiao, P., Zhong, Y., Wu, P., and Xu, L. (2022). The genus *Chrysanthemum*: Phylogeny, biodiversity, phytometabolites, and chemodiversity. *Frontiers in Plant Science, 13*, 973197, https://doi.org/10.3389/fpls.2022.973197.

Hegazi, E. S., Aml, R. M. J., Abdallatif, A. M., Thanaa, S. M. M., and Mona, K. M. M. (2021). Effect of silver nanoparticles, medium composition and growth regulators on *in vitro* propagation of picual olive cultivar. *Egyptian Journal of Chemistry, 64*(12), 6961–6969.

Huang, Y. W., Cambre, M., and Lee, H. J. (2017). The toxicity of nanoparticles depends on multiple molecular and physicochemical mechanisms. *International Journal of Molecular Sciences, 18*(12), 2702, https://doi.org/10.3390/ijms18122702.

Kereša, S., Mihovilović, A., Barić, M., Židovec, V., and Skelin, M. (2012). The micropropagation of chrysanthemums via axillary shoot proliferation and highly efficient plant regeneration by somatic embryogenesis. *African Journal of Biotechnology, 11*(22), 6027–6033, https://doi.org/10.5897/AJB10.1976.

Kim, D. H., Gopal, J., and Sivanesan, I. (2017). Nanomaterials in plant tissue culture: The disclosed and undisclosed. *RSC Advances, 7*, 36492, https://doi.org/10.1039/c7ra07025j.

Kumari, M. Khan, S. S., Pakrashi, S., Mukherjee, A., and Chandrasekaran, N. (2011). Cytogenetic and genotoxic effects of zinc oxide nanoparticles on root cells of *Allium cepa*. *Journal of Hazardous Materials, 190*(1–3), 613–621, https://doi.org/10.1016/j.jhazmat.2011.03.095.

Lema-Rumińska, J., Zalewska, M., and Sadoch, M. (2004). Radiomutants of chrysanthemum (*Dendranthema grandiflora* Tzvelev) of the Lady group: RAPD analysis of the genetic diversity. *Plant Breeding, 123*, 290–293, https://doi.org/10.1111/j.1439-0523.2004.00996.x.

Li, S., Liu, J., Wang, Y., Gao, Y., Zhang, Z., Xu, J., and Xing, G. (2021). Comparative physiological and metabolomic analyses revealed that foliar spraying with zinc oxide and silica nanoparticles modulates metabolite profiles in cucumber (*Cucumis sativus* L.). *Food and Energy Security, 10*, e269, https://doi.org/10.1002/fes3.269.

Lichtenthaler, H. K. (1987). Chlorophylls and carotenoids: Pigments of photosynthetic biomembranes. *Methods in Enzymology, 148*, 350–382, https://doi.org/10.1016/0076-6879(87)48036-1.

López-Reyes, A. Y., Rosas-Castor, J. M., Aragón-Piña, A., Lara-Martínez, E. M., Alfaro-Barbosa, J. M., and Leura-Vicencio, A. K. (2022). Zinc oxide nanoparticles and their effects in crops growth: Physical, biochemical and morphological point of views. *Journal of Plant Biology and Crop Research, 5*(2), 1066.

Mahendran, D., Geetha, N., and Venkatachalam, P. (2019). Role of silver nitrate and silver nanoparticles on tissue culture medium and enhanced the plant growth and development. In M. Kumar, A. Muthusamy, V. Kumar, and N. Bhalla-Sarin (Eds), *In vitro plant breeding towards novel agronomic traits* (pp. 59–74). Singapore: Springer, https://doi.org/10.1007/978-981-32-9824-8_4.

Majcher, A., Wiejak, J., Przybylski, J., Chudoba, T., and Wojnarowicz, J. (2013). A novel reactor for microwave hydrothermal scale-up nanopowder synthesis. *International Journal of Chemical Reactor Engineering, 11*, 361–368, https://doi.org/10.1515/ijcre-2012-0009.

Mazaheri-Tirani, M., and Dayani, S. (2020). *In vitro* effect of zinc oxide nanoparticles on *Nicotiana tabacum* callus compared to ZnO micro particles and zinc sulfate ($ZnSO_4$). *Plant Cell Tissue and Organ Culture, 140*, 279–289, https://doi.org/10.1007/s11240-019-01725-0.

Miler, N., Jędrzejczyk, I., Trafara, P., and Winiecki, J. (2023). Effect of high-energy ionizing radiation on the DNA content and genetic variation in chrysanthemum plants regenerated from irradiated ovaries. *Acta Scientiarium Polonorum Hortorum Cultus, 22*(4), 117–134, https://doi.org/10.24326/asphc.2023.4912.

Munir, T., Rizwan, M., Kashif, M., Shahzad, A., Ali, S., Amin, N., Zahid, R., Alam, M. F. E., and Imran, M. (2018). Effect of zinc oxide nanoparticles on the growth and Zn uptake in wheat (*Triticum aestivum* L.) by seed priming method. *Digest Journal of Nanomaterials and Biostructures, 13*(1), 315–323.

Murashige, T., and Skoog, F. (1962). A revised medium for rapid growth and bioassays with tobacco tissue cultures. *Physiologia Plantarum, 15*, 473–497, https://doi.org/10.1111/j.1399-3054.1962.tb08052.x.

Nalini, R. (2012). Micropropagation of chrysanthemum (*Chrysanthemum morifolium*) using shoot tip as explant. *International Journal of Food, Agriculture and Veterinary Sciences, 2*(2), 62–66.

Oraghi Ardebili, Z., and Sharifi, P. (2018). Growth and physiology of *Chrysanthemum morifolium* modified by the supplementations of various fertilizers. *Journal of Ornamental Plants, 8*(1), 49–56.

Panda, K. K., Golari, D., Venugopal, A., Achary, V. M. M., Phaomei, G., Parinandi, N. L., Sahu, H. K., and Panda, B. B. (2017). Green synthesized zinc oxide (ZnO) nanoparticles induce oxidative stress and DNA damage in *Lathyrus sativus* L. root bioassay system. *Antioxidants, 6*(2), 35, https://doi.org/10.3390/antiox6020035.

Pandey, A. C., Sanjay, S. S., and Yadav, R. S. (2010). Application of ZnO nanoparticles in influencing the growth rate of *Cicer arietinum. Journal of Experimental Nanoscience*, *5*(6), 488–497, https://doi.org/10.1080/17458081003649648.

Park, C. H., Chae, S. C., Park, S.-Y., Kim, J. K., Kim, Y. J., Chung, S. O., Arasu, M. V., Al-Dhabi, N. A., and Park, S. U. (2015). Anthocyanin and carotenoid contents in different cultivars of chrysanthemum (*Dendranthema grandiflorum* Ramat.) flower. *Molecules, 20*(6), 11090–11102, https://doi.org/10.3390/molecules200611090.

Parzymies, M. (2021). Nano-silver particles reduce contaminations in tissue culture but decrease regeneration rate and slows down growth and development of *Aldrovanda vesiculosa* explants. *Applied Sciences, 11*(8), 3653, https://doi.org/10.3390/app11083653.

Patlolla, A. K., Berry, A., May, L., and Tchounwou, P. B. (2012). Genotoxicity of silver nanoparticles in *Vicia faba*: A pilot study on the environmental monitoring of nanoparticles. *International Journal of Environmental Research and Public Health, 9*, 1649, https://doi.org/10.3390/ijerph9051649.

Plaksenkova, I., Kokina, I., Petrova, A., Jermaļonoka, M., Gerbreders, V., and Krasovska, M. (2020). The impact of zinc oxide nanoparticles on cytotoxicity, genotoxicity, and miRNA expression in barley (*Hordeum vulgare* L.) seedlings. *Scientific World Journal, 2020*, Article ID 6649746, 13 p, https://doi.org/10.1155/2020/6649746.

Pokrowiecki, R., Wojnarowicz, J., Zareba, T., Koltsov, I., Lojkowski, W., Tyski, S., Mielczarek, A., and Zawadzki, P. (2019). Nano-particles and human saliva: A step towards drug delivery systems for dental and craniofacial biomaterials. *International Journal of Nanomedicine, 14*, 9235–9257, https://doi.org/10.2147/IJN.S221608.

Rani, S., Kumar, P., Dahiya, P., Dang, A. S., and Suneja, P. (2022). Biogenic synthesis of zinc nanoparticles, their application, and toxicity prospects. *Frontiers in Microbiology, 13*, 824427, https://doi.org/10.3389/fmicb.2022.824427.

Regni, L., Del Buono, D., Micheli, M., Facchin, S. L., Tolisano, C., Del Pino, A. M., and Proietti, P. (2022). Biostimulant effects of biogenic ZnO nanoparticles on *in vitro* explants proliferation of olive cultivar 'Moraiolo'. *Acta Horticulturae, 1334*, 123–128, https://doi.org/10.17660/ActaHortic.2022.1344.19.

Regni, L., Micheli, M., Del Pino, A. M., Palmerini, C. A., D'amato, R., Facchin, S. L., Famiani, F., Peruzzi, A., Mairech, H., and Proietti, P. (2021). The first evidence of the beneficial effects of se-supplementation on *in vitro* cultivated olive tree explants. *Plants, 10*(8), 1630, https://doi.org/10.3390/plants10081630.

Sadak, M. S., and Bakry, B. A. (2020). Zinc-oxide and nano ZnO oxide effects on growth, some biochemical aspects, yield quantity, and quality of flax (*Linum uitatissimum* L.) in absence and presence of compost under sandy soil. *Bulletin of the National Research Centre, 44*, 98, https://doi.org/10.1186/s42269-020-00348-2.

Salachna, P., Byczyńska, A., Zawadzińska, A., Piechocki, R., and Mizielińska, M. (2019). Stimulatory effect of silver nanoparticles on the growth and flowering of potted oriental lilies. *Agronomy, 9*(10), 610, https://doi.org/10.3390/agronomy9100610.

Salachna, P., Mizielińska, M., Płoszaj-Witkowska, B., and Jaszczak, A. (2021). Zinc oxide nanoparticles enhanced biomass and zinc content and induced changes in biological properties of red *Perilla frutescens*. *Materials, 14(20)*, 6182, https://doi.org/10.3390/ma14206182.

Sarkhosh, S., Kahrizi, D., Darvishi, E., Tourang, M., Haghighi-Mood, S., Vahedi, P., and Ercisli, S. (2022). Effect of zinc oxide nanoparticles (ZnO-NPs) on seed germination characterictics in two *Brassicaceae* family species: *Camelina sativa* and *Brassica napus* L. *Journal of Nanomaterials, 2022*, Article ID 1892759, 15 p, https://doi.org/10.1155/2022/1892759.

Shafique, S., Jabeen, N., Ahmad, K. S., Irum, S., Anwaar, S., Ahmad, N., Alam, S., Ilyas, M., Khan, T. F., and Hussain, S. Z. (2020). Green fabricated zinc oxide nanoformulated media enhanced callus induction and regeneration dynamics of *Panicum virgatum* L. *PLOS One, 15*(7), e0230464, https://doi.org/10.1371/journal.pone.0230464.

Shibata, M., Kishimoto, S., Hirai, M., Aida, R., and Ikeda, I. (1998). Analysis of the periclinal chimeric structure of chrysanthemum sports by random amplified polymorphic DNA. *Acta Horticulturae, 454*, 347–353, https://doi.org/10.17660/ActaHortic.1998.454.41.

Shin, J., Bae, S., and Seo, P. J. (2020). De novo shoot organogenesis during plant regeneration. *Journal of Experimental Botany, 71*(1), 63–72, https://doi.org/10.1093/jxb/erz395.

Sohail K. K., Kemmerling, B., Shutaywi, M., and Mashwani Zu, R. (2020). Nano zinc elicited biochemical characterization, nutritional assessment, antioxidant enzymes and fatty acid profiling of rapeseed. *PLOS One, 15*(11), e0241568, https://doi.org/10.1371/journal.pone.0241568.

Sorahinobar, M., Deldari, T., Nazem Bokaeei, Z., and Mehdina, A. (2022). Effect of zinc nanoparticles on the growth and biofortification capability of mungbean (*Vigna radiata*) seedlings. *Biologia, 78*, 951–960, https://doi.org/10.1007/s11756-022-01269-3.

Speranza, A., Crinelli, R., Scoccianti, V., Taddei, A. R., Iacobucci, M., Bhattacharya, P. and Ke, P. C. (2013). In vitro toxicity of silver nanoparticles to kiwifruit pollen exhibits peculiar traits beyond the cause of silver ion release. *Environmental Pollution*, 179, 258–267, https://doi.org/10.1016/j.envpol.2013.04.021.

Su, J., Jiang, J., Zhang, F., Liu, Y., Ding, L., Chen, S., and Chen, F. (2019). Current achievements and future prospects in the genetic breeding of chrysanthemum: A review. *Horticulture Research*, 6, 109, https://doi.org/10.1038/s41438-019-0193-8.

Sun, L., Wang, Y., Wang, R., Wang, R., Zhang, P., Ju, Q., and Xu, J. (2020). Physiological, transcriptomic, and metabolomic analyses reveal zinc oxide nanoparticles modulate plant growth in tomato. *Environmental Science: Nano, 7*, 3587–3604, https://doi.org/10.1039/D0EN00723D.

Tariq, M., Mohammad, K. N., Ahmed, B., Siddiqui, M. A., and Lee, J. (2022). Biological synthesis of silver nanoparticles and prospects in plant disease management. *Molecules, 27*(15), 4754, https://doi.org/10.3390/molecules27154754.

Thunugunta, T., Channa Reddy, A., Kodthalu Seetharamaiah, S., Ramanna Hunashikatti, L., Gowdra Chandrappa, S., Cherukatu Kalathil, N., And Dhoranapalli Chinnappa Reddy, L. R. (2018). Impact of zinc oxide nanoparticles on eggplant (*S. melongena*): Studies on growth and the accumulation of nanoparticles. *IET Nanobiotechnology, 12*(6), 706–713, https://doi.org/10.1049/iet-nbt.2017.0237.

Tripathi, D. K., Shweta Singh, S., Singh, S., Pandey, R., Singh, V. P., Sharma, N. C., Prasad, S. M., Dubey, N. K., and Chauhan, D. K. (2016). An overview on manufactured nanoparticles in plants: Uptake, translocation, accumulation and phytotoxicity. *Plant Physiology and Biochemistry, 110*, 2–12, https://doi.org/10.1016/j.plaphy.2016.07.030.

Tymoszuk, A., and Kulus, D. (2022). Effect of silver nanoparticles on the *in vitro* regeneration, biochemical, genetic, and phenotype variation in adventitious shoots produced form leaf explants in chrysanthemum. *International Journal of Molecular Sciences*, *23*(13), 7406, https://doi.org/10.3390/ijms23137406.

Tymoszuk, A., and Miler, N. (2019). Silver and gold nanoparticles impact on *in vitro* adventitious organogenesis in chrysanthemum, gerbera and Cape Primrose. *Scientia Horticulturae, 257*, 108766, https://doi.org/10.1016/j.scienta.2019.108766.

Tymoszuk, A., Sławkowska, N., Szałaj, U., Kulus, D., Antkowiak, M., and Wojnarowicz, J. (2022). Synthesis, characteristics, and effect of zinc oxide and silver nanoparticles on the *in vitro* regeneration and biochemical profile of chrysanthemum adventitious shoots. *Materials, 15*(22), 8192, https://doi.org/10.3390/ma15228192.

Wang, X. P., Li, Q. Q., Pei, Z. M., and Wang, S. C. (2018). Effects of zinc oxide nanoparticles on the growth, photosynthetic traits, and antioxidative enzymes in tomato plants. *Biologia Plantarum, 62*, 801–808, https://doi.org/10.1007/s10535-018-0813-4.

Williams, J. G. K., Kubelik, A. R., Livak, K. J., Rafalski, J. A., and Tingey, S. V. (1990). DNA polymorphisms amplified by arbitrary primers are useful as genetic markers. *Nucleic Acids Research, 18*, 6531–6535, https://doi.org/10.1093/nar/18.22.6531.

Wojnarowicz, J., Chudoba, T., and Lojkowski, W. (2020). A review of microwave synthesis of zinc oxide nanomaterials: Reactants, process parameters and morphologies. *Nanomaterials, 10*(6), 1086, https://doi.org/10.3390/nano10061086.

Wojnarowicz, J., Chudoba, T., Gierlotka, S., Sobczak, K., and Lojkowski, W. (2018). Size control of cobalt-doped ZnO nanoparticles obtained in microwave solvothermal synthesis. *Crystals, 8*(4), 179, https://doi.org/10.3390/cryst8040179.

Wolff, K. (1996). RAPD analysis of sporting and chimerism in chrysanthemum. *Euphytica, 89*, 159–164, https://doi.org/10.1007/BF00034601.

Zalewska, M., Antkowiak, M., and Tymoszuk, A. (2012). Micropropagation of *Ajania pacifica* (Nakai) Bremer et Humphries with single-node method. *Nauka Przyroda Technologie, 6*(1), #10.

Zalewska, M., Tymoszuk, A., and Miler, N. (2011). New chrysanthemum cultivars as a result of *in vitro* mutagenesis with the application of different explants types. *Acta Scientiarum Polonorum Hortorum Cultus, 10*(2), 109–123.

Zhang, H., Wang, R., Chen, Z., Cui, P., Yang, Y., and Zhang, H. (2021). The effect of zinc oxide nanoparticles for enhancing rice (*Oryza sativa* L.) yield and quality. *Agriculture, 11*(12), 1247, https://doi.org/10.3390/agriculture11121247.

Received: October 31, 2023; accepted: January 16, 2024

SUPPLEMENTARY MATERIALS

Supplementary Table S1. Composition of the precursor solution used for synthesis

Sample name	Ethylene glycol volume (mL)	Weight of zinc acetate dihydrate (g)	Weight of silver acetate anhydrous (g)	Final water content of the precursor solution (weight %)
ZnO NPs (1.5% H_2O)	525	35 g	0	1.5
ZnO NPs (6% H_2O)				6
ZnO + 0.1% Ag NPs (1.5% H_2O)			0.0266	1.5
ZnO + 0.1% Ag NPs (6% H_2O)			0.0266	6
ZnO + 1% Ag NPs (1.5% H_2O)			0.2689	1.5
ZnO + 1% Ag NPs (6% H_2O)			0.2689	6

NPs, nanoparticles.

Supplementary Table S2. Characteristics of samples

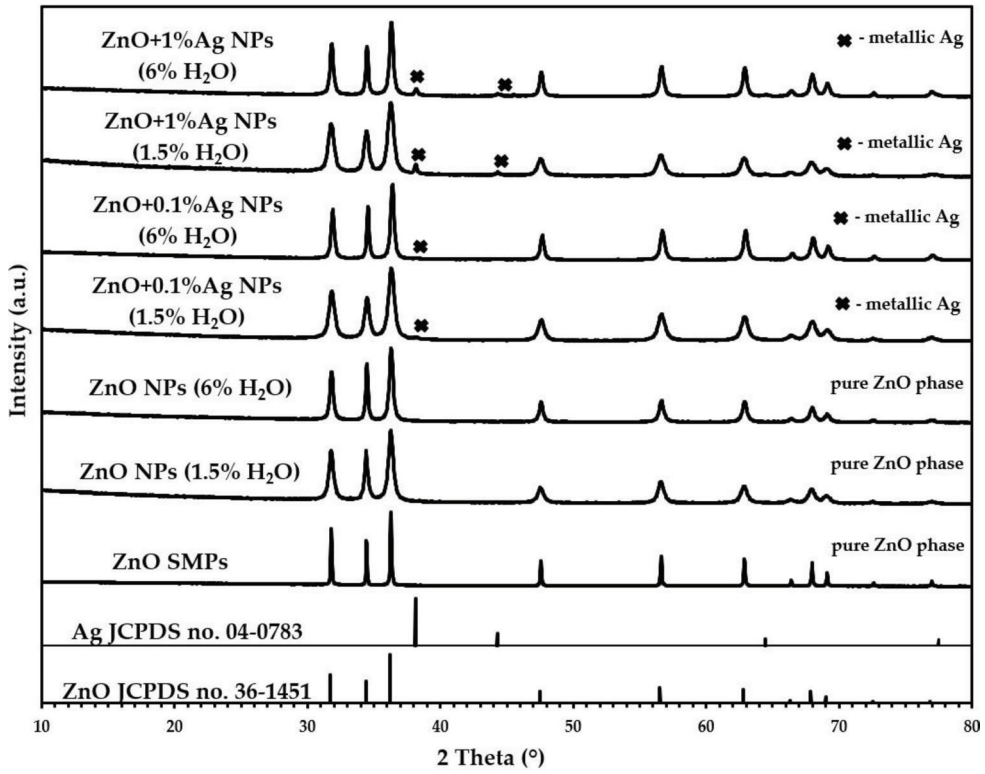
Sample name	Skeleton density, $\rho_s \pm \sigma$ ($g \cdot cm^{-3}$)	SSA, a_s ($m^2 \cdot g^{-1}$)	Average particle size from SSA BET, $d \pm \sigma$ (nm)	Average crystallite size, Scherrer equation, $d \pm \sigma$ (nm)
ZnO SMPs	5.59 ± 0.03	4.5	240 ± 30	124 ± 11
ZnO NPs (1.5% H_2O)	5.09 ± 0.06	48.4	25 ± 2	31 ± 8
ZnO NPs (6% H_2O)	5.38 ± 0.05	17.2	65 ± 6	40 ± 10
ZnO + 0.1% Ag NPs (1.5% H_2O)	5.16 ± 0.07	40.0	29 ± 2	17 ± 5 (ZnO) 31 ± 10 (Ag)
ZnO + 0.1% Ag NPs (6% H_2O)	5.37 ± 0.06	14.2	79 ± 2	39 ± 12 (ZnO) 31 ± 10 (Ag)
ZnO + 1% Ag NPs (1.5% H_2O)	5.05 ± 0.05	44.4	27 ± 2	22 ± 3 (ZnO) 45 ± 20 (Ag)
ZnO + 1% Ag NPs (6% H_2O)	5.31 ± 0.09	21.4	53 ± 2	35 ± 5 (ZnO) 31 ± 15 (Ag)

BET, Brunauer–Emmett–Teller; NPs, nanoparticles; SMPs, submicron particles; SSA, specific surface area.

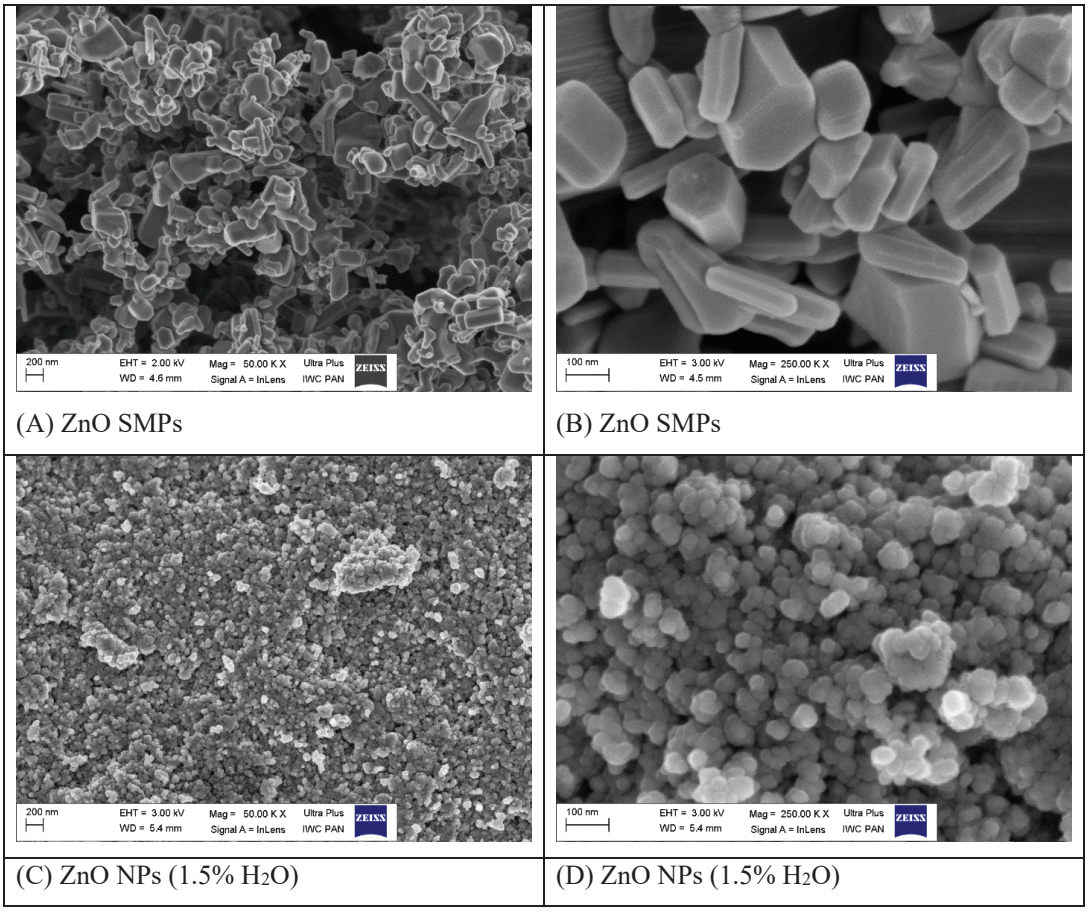
Supplementary Table S3. Results of the analysis of the chemical composition of the sample

Sample name	Actual dopant content (mol%)		Nominal composition (mol%)		Weight content of ZnO and Ag in 100 mg of sample (mg)	
	Zinc	Silver	Zinc	Silver	ZnO	Ag
ZnO + 0.1% Ag NPs (1.5% H_2O)	99.91 ± 0.04	0.09 ± 0.04	99.9	0.1	99.881	0.119
ZnO + 0.1% Ag NPs (6% H_2O)	99.85 ± 0.06	0.15 ± 0.06	99.9	0.1	99.801	0.199
ZnO + 1% Ag NPs (1.5% H_2O)	99.05 ± 0.20	0.95 ± 0.20	99.00	1.00	98.745	1.255
ZnO + 1% Ag NPs (6% H_2O)	98.95 ± 0.20	1.05 ± 0.20	99.00	1.00	98.613	1.387

The method of analysis was EDS.
EDS, energy-dispersive spectrometry; NPs, nanoparticles.



Supplementary Figure S1. X-ray diffraction patterns of samples.



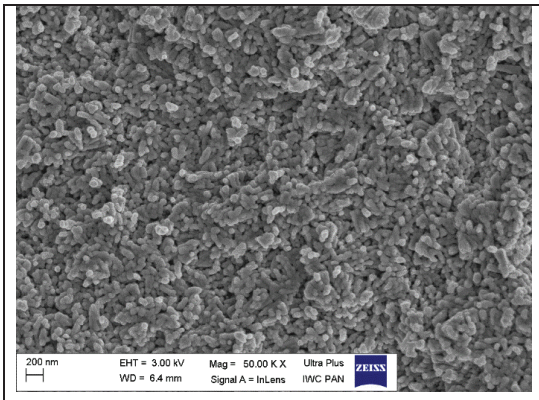
(A) ZnO SMPs

(B) ZnO SMPs

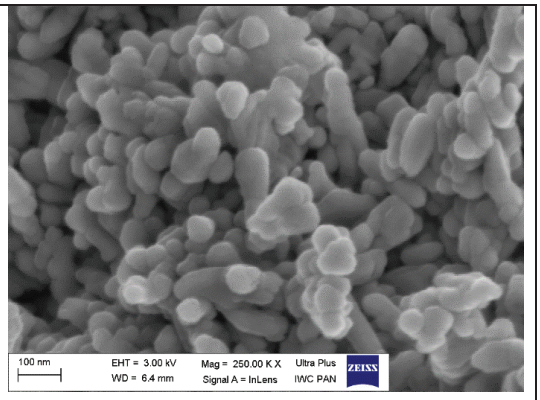
(C) ZnO NPs (1.5% H_2O)

(D) ZnO NPs (1.5% H_2O)

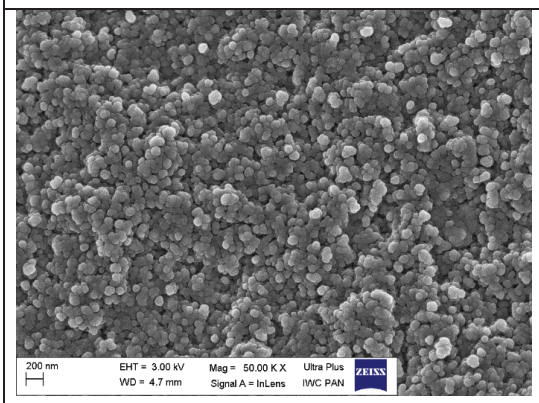
Supplementary Figure S2. Continued.



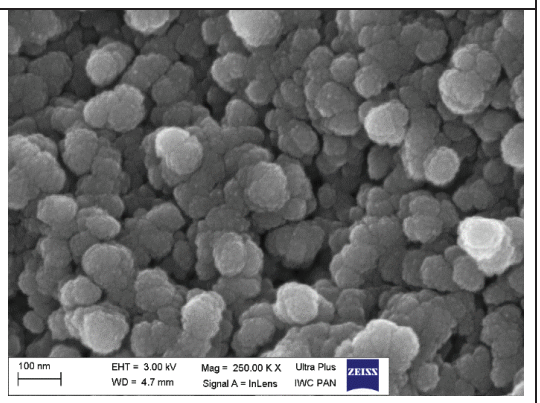
(E) ZnO NPs (6% H_2O)



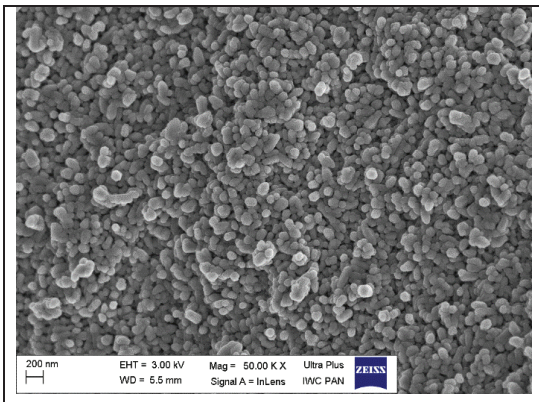
(F) ZnO NPs (6% H_2O)



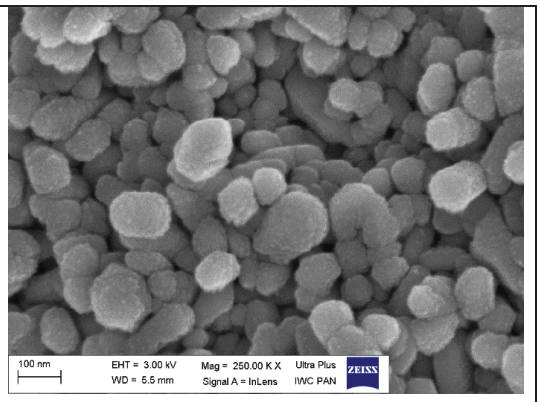
(G) ZnO + 0.1% Ag NPs (1.5% H_2O)



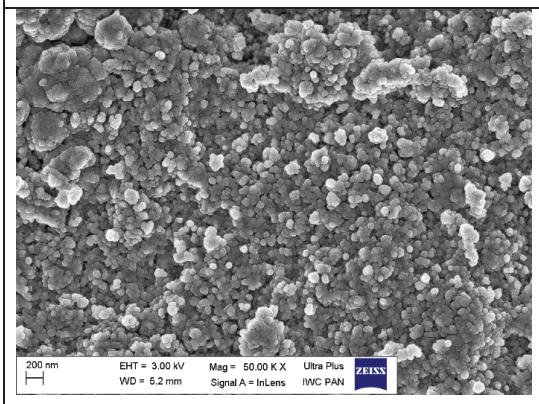
(H) ZnO + 0.1% Ag NPs (1.5% H_2O)



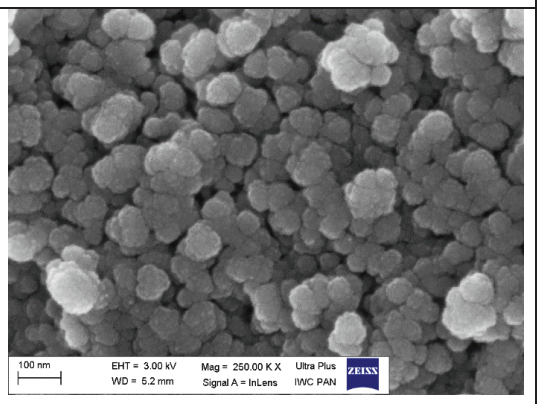
(I) ZnO + 0.1% Ag NPs (6% H_2O)



(J) ZnO + 0.1% Ag NPs (6% H_2O)'

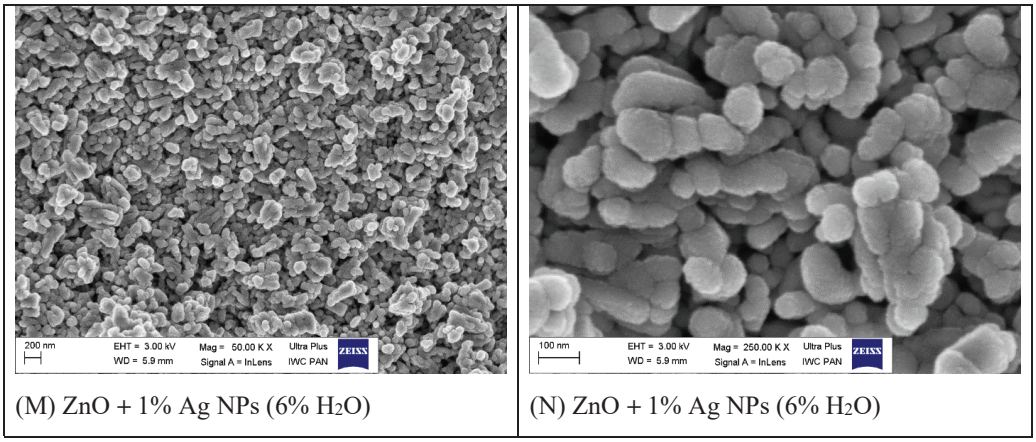


(K) ZnO + 1% Ag NPs (1.5% H_2O)



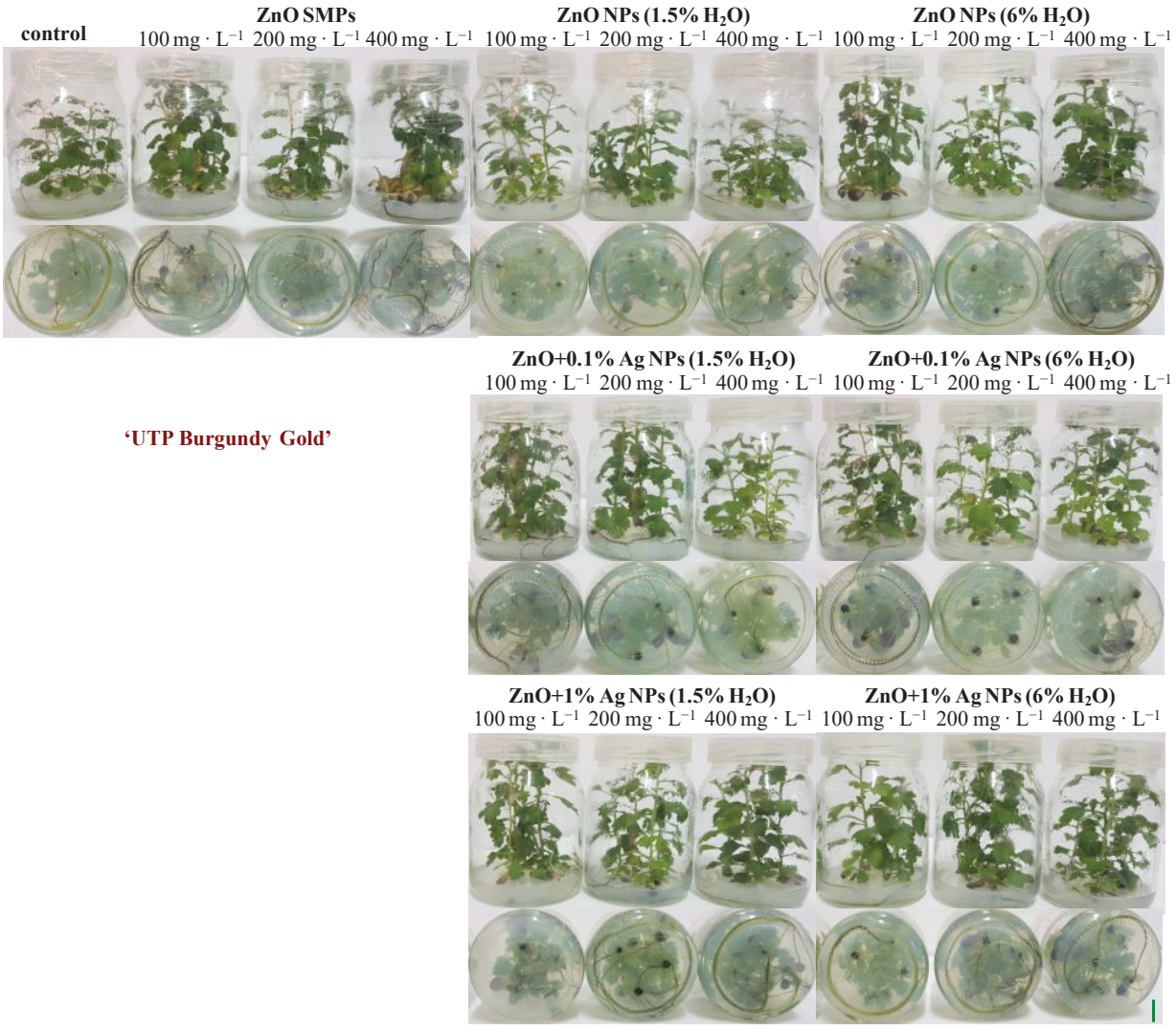
(L) ZnO + 1% Ag NPs (1.5% H_2O)

Supplementary Figure S2. Continued.

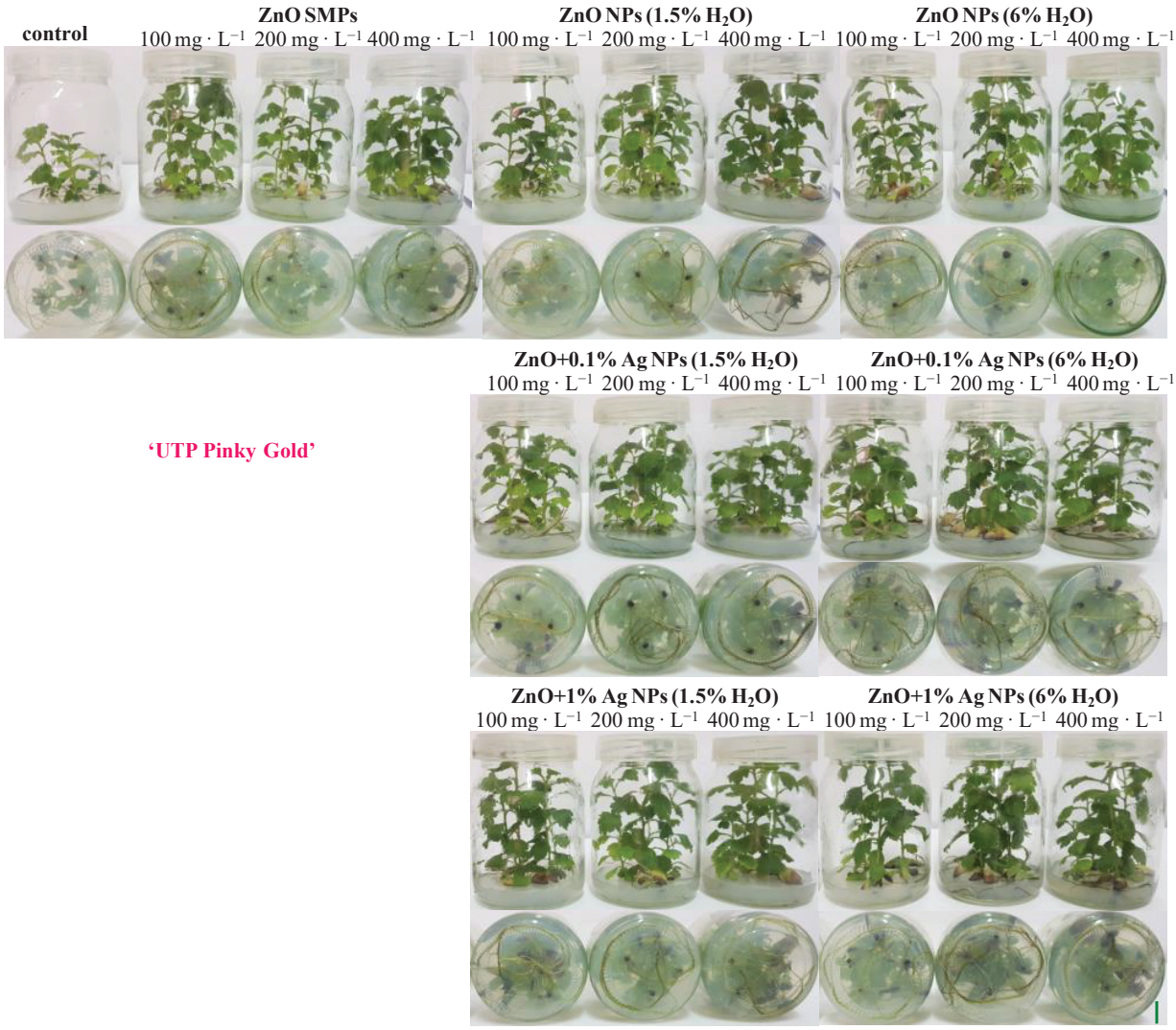


(M) ZnO + 1% Ag NPs (6% H_2O) (N) ZnO + 1% Ag NPs (6% H_2O)

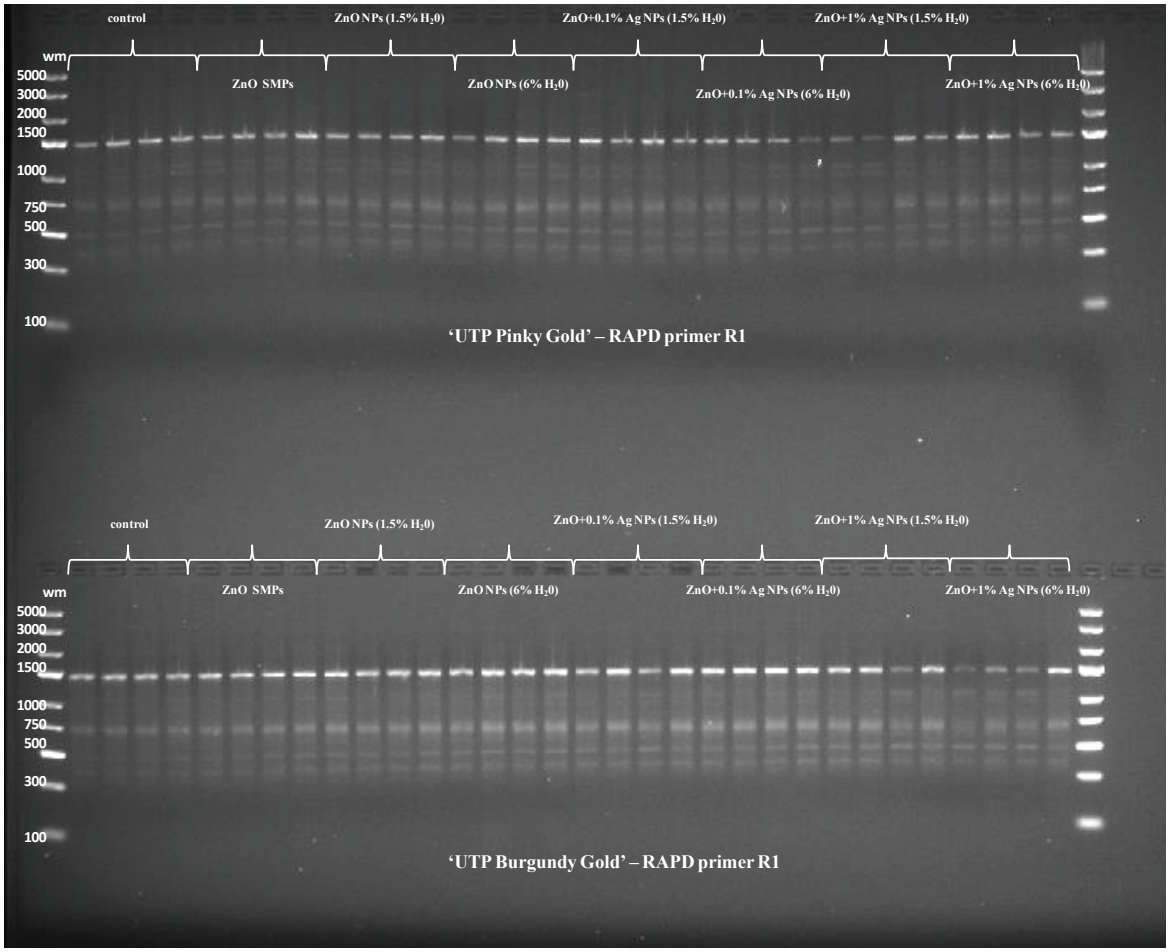
Supplementary Figure S2. SEM images of samples: (A, B) ZnO SMPs; (C, D) ZnO NPs (1.5% H_2O); (E, F) ZnO NPs (6% H_2O); (G, H) ZnO + 0.1% Ag NPs (1.5% H_2O); (I, J) ZnO + 0.1% Ag NPs (6% H_2O); (K, L) ZnO + 1% Ag NPs (1.5% H_2O); (M, N) ZnO + 1% Ag NPs (6% H_2O) images taken with the immersion lens detector. NPs, nanoparticles; SMPs, submicron particles.

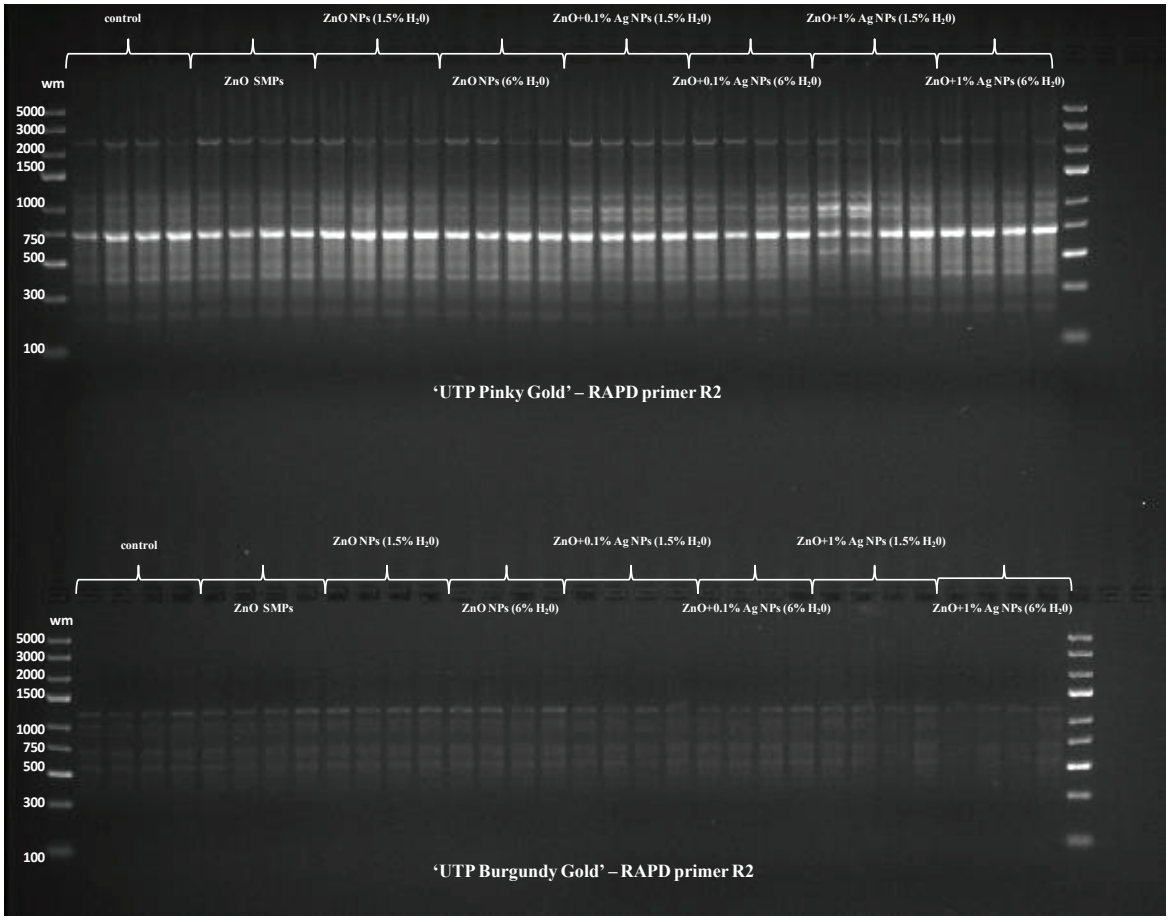


Supplementary Figure S3. Continued.

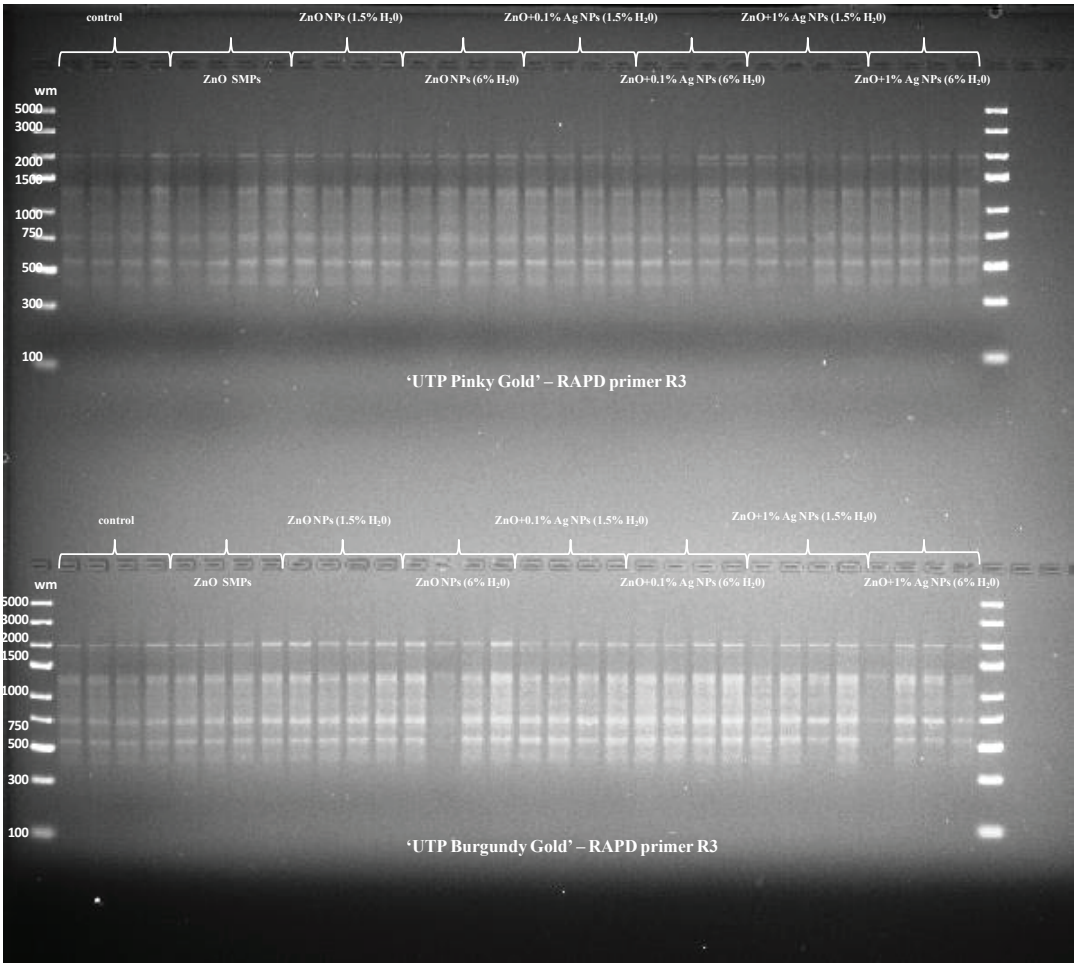


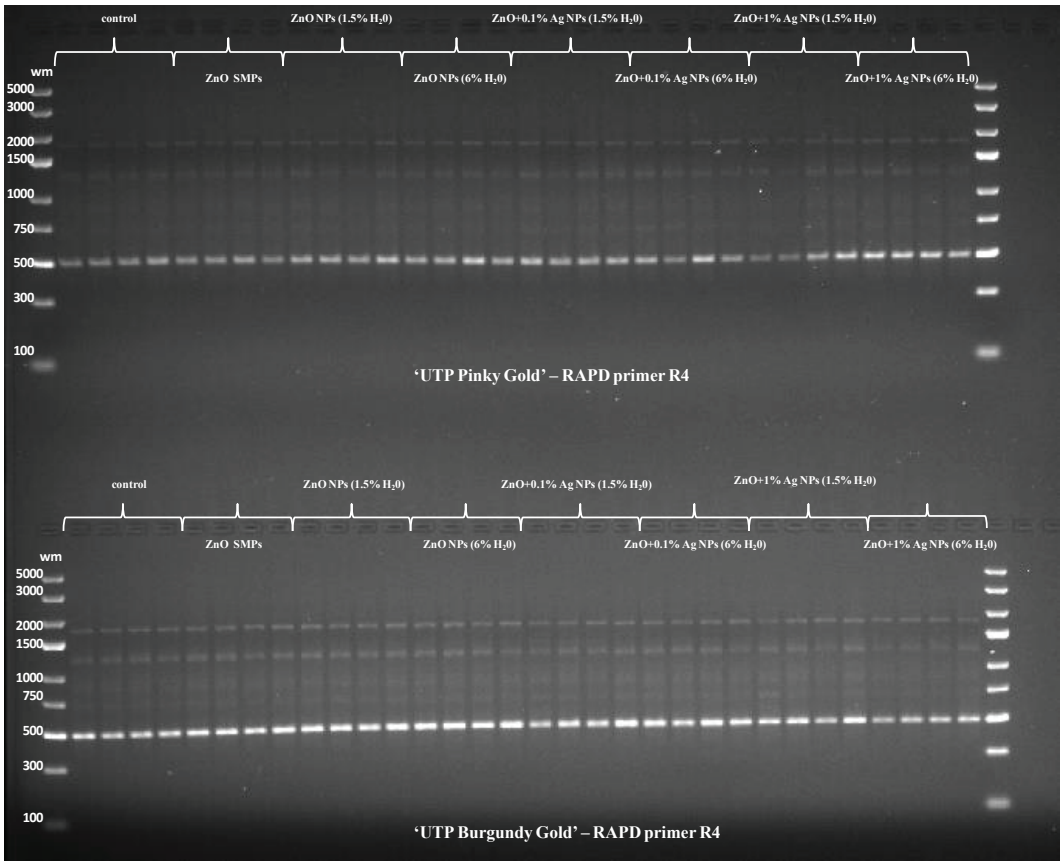
Supplementary Figure S3. *Chrysanthemum* × *morifolium* 'UBG' and 'UPG' shoot and root systems developed from node explants cultured *in vitro* for 10 weeks on the modified MS medium, depending on the ZnO SMPs/ZnO NPs/ZnO + Ag NPs treatment; bar = 1 cm. MS, Murashige and Skoog; NPs, nanoparticles; SMPs, submicron particles; UBG, 'UTP Burgundy Gold'; UPG, 'UTP Pinky Gold'.



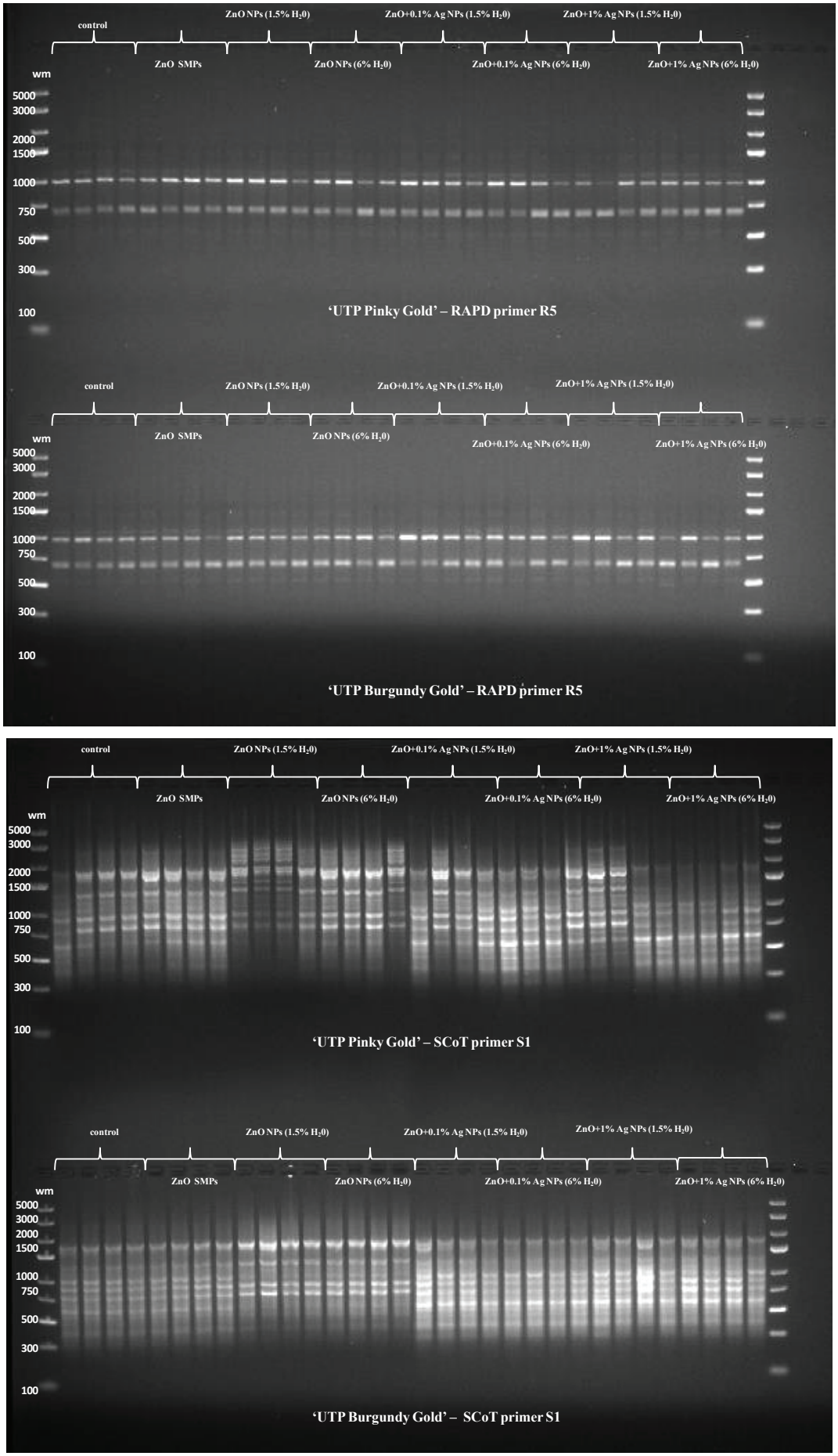


Supplementary Figure S4. Continued.

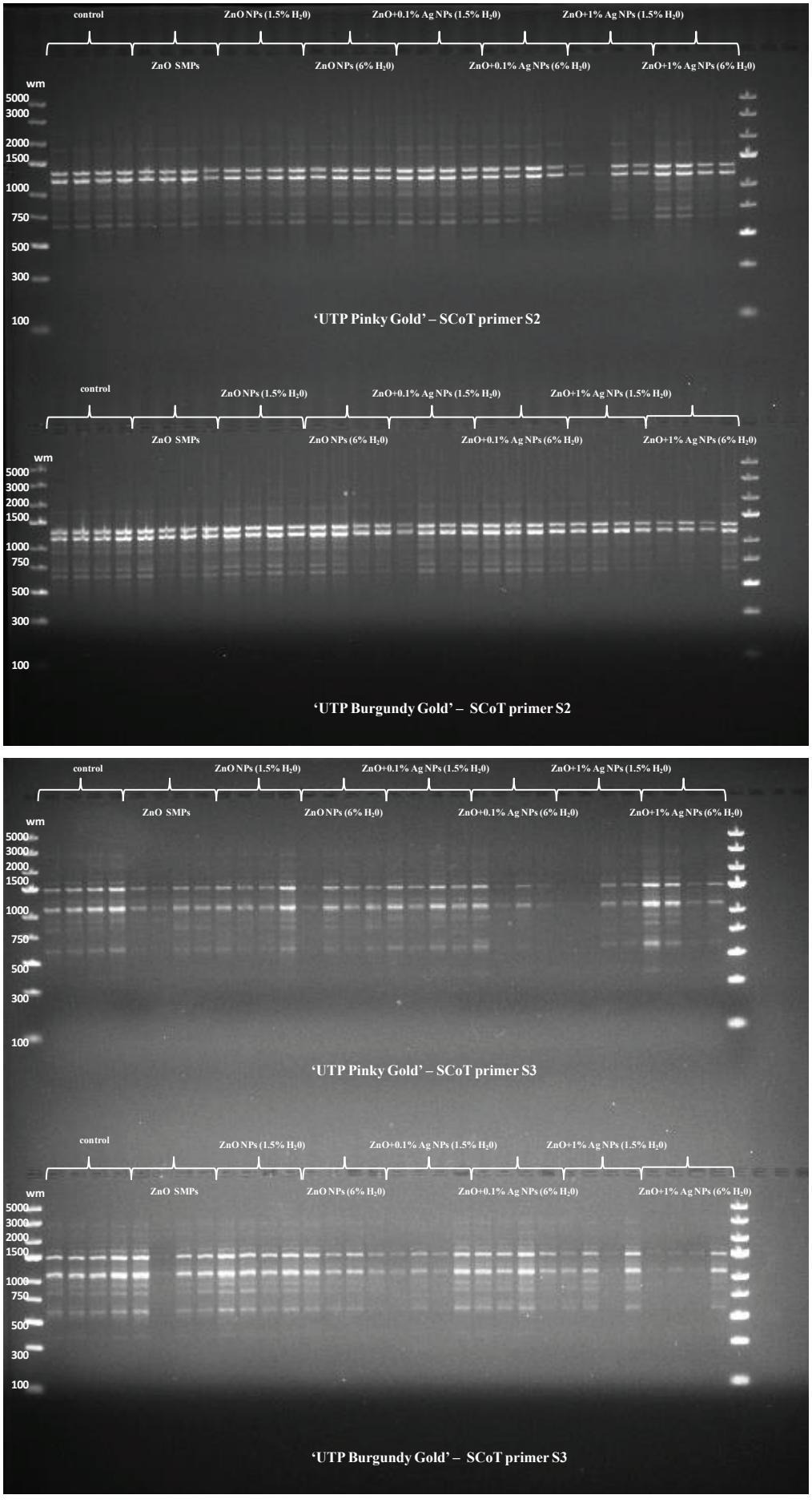




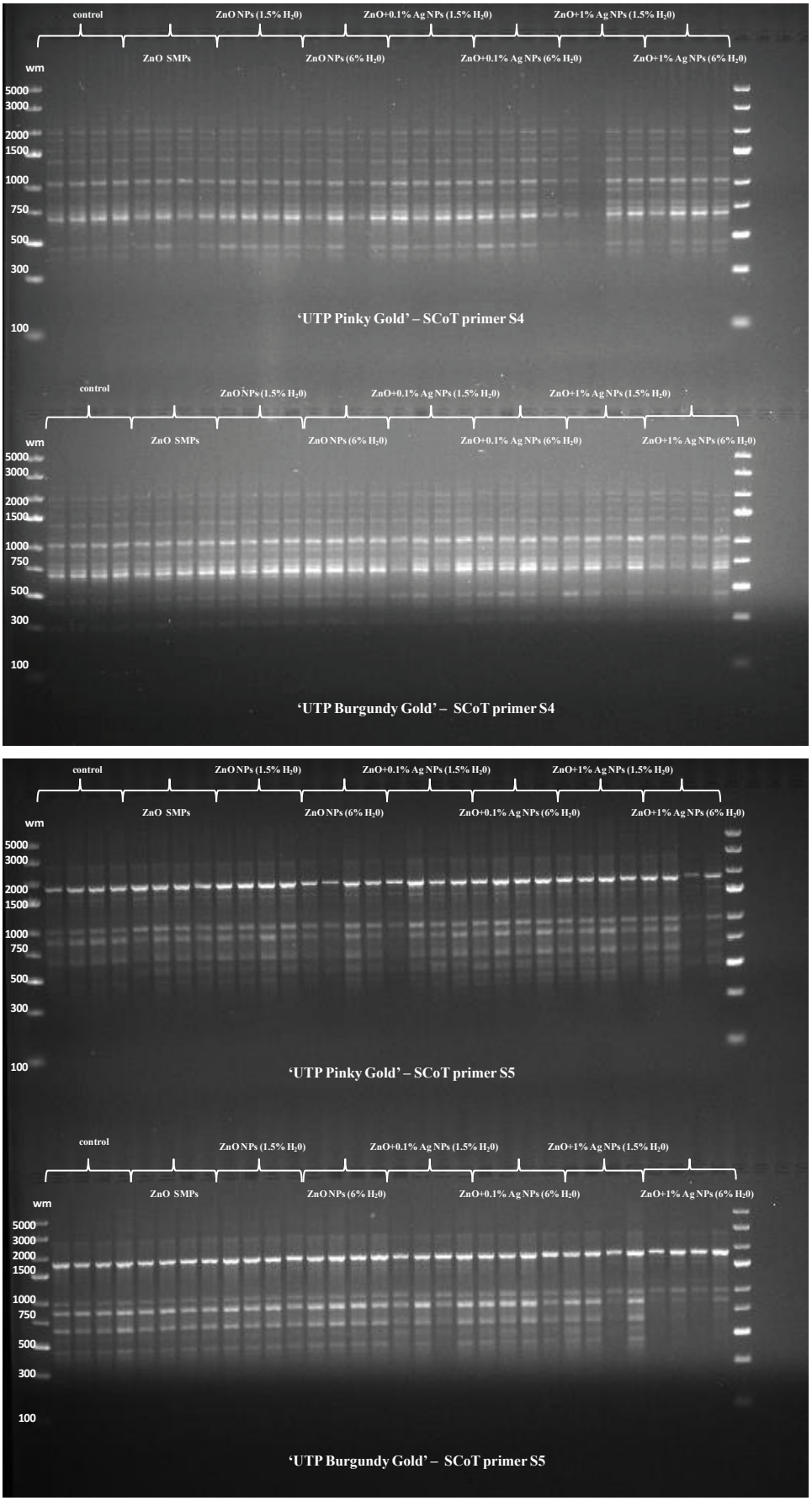
Supplementary Figure S4. Continued.



Supplementary Figure S4. Continued.



Supplementary Figure S4. Continued.



Supplementary Figure S4. RAPD and SCoT band profiles of the control and 400 mg · L^{-1} ZnO SMPs/ZnO NPs/ZnO + Ag NPs-treated plantlets of *Chrysanthemum* × *morifolium* 'UBG' and 'UPG'. Outermost lanes (wm) are DNA bp weight markers. NPs, nanoparticles; RAPD, randomly amplified polymorphic DNA; SCoT, start codon targeted polymorphism; SMPs, submicron particles; UBG, 'UTP Burgundy Gold'; UPG, 'UTP Pinky Gold'.